HHS Public Access

Author manuscript

Neuron. Author manuscript; available in PMC 2018 December 20.

Published in final edited form as:

Neuron. 2017 December 20; 96(6): 1327–1341.e6. doi:10.1016/j.neuron.2017.11.037.

Drp1 mitochondrial fission in D1 neurons mediates behavioral and cellular plasticity during early cocaine abstinence

Ramesh Chandra[1,8], **Michel Engeln**[1,8], **Christopher Schiefer**[1], **Mary H. Patton**[2], **Jennifer A. Martin**[3], **Craig T. Werner**[3], **Lace M. Riggs**[1], **T. Chase Francis**[1], **Madeleine McGlincy**[1], **Brianna Evans**[1], **Hyungwoo Nam**[1], **Shweta Das**[1], **Kasey Girven**[1], **Prasad Konkalmatt**[4], **Amy M. Gancarz**[3], **Sam A. Golden**[5], **Sergio D. Iñiguez**[6], **Scott J. Russo**[5], **Gustavo Turecki**[7], **Brian N. Mathur**[2], **Meaghan Creed**[2], **David M. Dietz**[3], and **Mary Kay Lobo**[1,*]

[1]Department of Anatomy and Neurobiology, University of Maryland School of Medicine, Baltimore, MD, USA

[2]Department of Pharmacology, University of Maryland School of Medicine, Baltimore, MD, USA

[3]Department of Pharmacology and Toxicology, The Research Institution on Addictions, State University of New York at Buffalo, Buffalo, NY, USA

[4]Division of Renal Diseases and Hypertension, The George Washington University, Washington, D.C, USA

[5]Fishberg Department of Neuroscience and Friedman Brain Institute, Graduate School of Biomedical Sciences at the Icahn School of Medicine at Mount Sinai, New York, New York, USA

[6]Department of Psychology, University of Texas at El Paso, El Paso, Texas, USA

[7]McGill Group for Suicide Studies, Douglas Mental Health University Institute, McGill University, Montréal, Québec, Canada

Summary

Altered brain energy homeostasis is a key adaptation occurring in the cocaine-addicted brain but the effect of cocaine on the fundamental source of energy, mitochondria, is unknown. We demonstrate an increase of dynamin-related protein-1 (Drp1), the mitochondrial fission mediator, in nucleus accumbens (NAc) after repeated cocaine exposure and in cocaine dependent individuals. Mdivi-1, a demonstrated fission inhibitor, blunts cocaine seeking and locomotor

[*]**To whom correspondence should be addressed (Corresponding/Lead contact):** Mary Kay Lobo, PhD, Department of Anatomy and Neurobiology, University of Maryland School of Medicine, 20 Penn Street, HSF II Rm S251, Baltimore, MD, 21201, USA, mklobo@som.umaryland.edu.

[8]These two contributed equally to the study.

Author contribution

R.C., M.E., C.S., M.H.P, J.A.M., C.T.W, L.M.R, T.C.F., M.M.G, B.B.E., H.N., S.D., K.G., P.K., A.M.G., S.A.G., M.C., B.N.M., and M.K.L. performed experiments. G.T. and S.R. provided postmortem human tissue and cDNA. R.C., M.E., M.K.L, D.M.D., S.I., B.N.M. and M.C. designed experiments. R.C., M.E., and M.K.L wrote the manuscript.

All authors report no biomedical financial interests or potential conflicts of interest.

sensitization, while blocking c-Fos induction and excitatory input onto dopamine receptor-1 (D1) containing NAc medium spiny neurons (MSNs). Drp1 and fission promoting Drp1 are increased in D1-MSNs, consistent with increased smaller mitochondria in D1-MSN dendrites after repeated cocaine. Knockdown of Drp1 in D1-MSNs blocks drug seeking after cocaine self-administration, while enhancing the fission promoting Drp1 enhances seeking after long-term abstinence from cocaine. We demonstrate a role for altered mitochondrial fission in the NAc, during early cocaine abstinence, suggesting potential therapeutic treatment of disrupting mitochondrial fission in cocaine addiction.

Introduction

Brain energy homeostasis is perturbed in cocaine abuse and after cocaine exposure. This includes alterations in glucose metabolism, oxidative stress, and cellular respiration, as well as imbalanced glutamate homeostasis (Cunha-Oliveira et al., 2013; Dietrich et al., 2005; Jang et al., 2015; Kalivas, 2009; Pomierny-Chamiolo et al., 2013; Volkow et al., 1991). Despite these studies, there is minimal investigation into mitochondria, the fundamental component of energy homeostasis, in select brain reward regions in motivation for cocaine or other drugs of abuse. Previous work demonstrates increased transcripts of molecules important for mitochondria function in postmortem prefrontal cortex of cocaine dependents (Lehrmann et al., 2003). Additionally, recent transcriptional profiling of the nucleus accumbens (NAc), a major brain reward nucleus, demonstrates enriched gene ontology of mitochondrial related transcripts after repeated cocaine (Feng et al., 2014). Further, in vitro application of cocaine to brain mitochondria, alters mitochondrial complex 1, mitochondrial respiration, and mitochondrial membrane potential (Cunha-Oliveira et al., 2013).

Recent studies demonstrate mitochondria dysfunction occurs in diseased motivational states including depression, bipolar disorder, anxiety, and stress response (Cai et al., 2015; CONVERGE consortium, 2015; Hollis et al., 2015; Manji et al., 2012; Picard et al., 2015; van der Kooij., et al 2017). For instance, BCL-2 function in the brain, which plays a role in mitochondrial Ca^{2+} homeostasis, is linked to mood disorders, and mood stabilizing agents can upregulate BCL-2 (Manji et al., 2012). Furthermore, stress and anxiety are associated with mitochondrial dysfunction: mutations in mitochondrial genes during acute stress can impact pathophysiological mechanisms mediated by stress (Picard et al., 2015), highly-anxious animals exhibit reduced mitochondrial complex proteins in the NAc (Hollis et al., 2015), and intra-NAc infusion of a D1 antagonist facilitates social dominance while increasing mitochondrial respiration (van der Kooij., et al 2017). Despite these insights into mitochondrial function in diseased motivational states, mitochondrial dynamics have not yet been examined in dysfunctional motivation. However, recent studies have examined mitochondrial dynamics in learning and memory and in a naturally rewarding behavior exercise (Hara et al., 2014; Steib et al., 2014). Mitochondrial morphology in prefrontal cortex presynaptic boutons is correlated with working memory performance (Hara et al., 2014). Additionally, exercise increases mitochondrial content and the presence of mitochondria in dendritic segments in newly developed neurons (Steib et al., 2014).

Mitochondria undergo dynamic processes including fission, the process of mitochondrial division, and fusion, the process of mitochondrial elongation (Detmer and Chan, 2007; Friedman and Nunnari, 2014; Westermann, 2010). These processes are critical for maintenance of mitochondrial function and cellular quality control. To provide insight into the effects of cocaine on mitochondrial dynamics, we examined mitochondrial fission and fusion molecules including dynamin-related protein 1 (Drp1), a mediator of mitochondrial fission (Detmer and Chan, 2007; Friedman and Nunnari, 2014; Westermann, 2010), in the NAc of animals receiving repeated cocaine and in cocaine dependents. We further examined the two main nucleus accumbens (NAc) projection medium spiny neuron (MSN) subtypes, those enriched in dopamine D1 vs. D2 receptors. These two MSN subtypes display critical but often differential roles in psychostimulant-mediated behaviors (Calipari et al., 2016; Ferguson et al., 2011; Hikida et al., 2010; Lobo et al., 2010; Lobo and Nestler, 2011; Smith et al., 2013). Previous studies demonstrate differential plasticity, signaling, and molecular processes in D1-MSNs vs. D2-MSNs with chronic cocaine (Bock et al., 2013; Chandra et al., 2015; Graziane et al., 2016; Heiman et al., 2008; Kim et al., 2011; Lobo et al., 2010; Lobo et al., 2013; MacAskill et al., 2014; Pascoli et al., 2014). Given these findings, it is plausible that these MSNs have different energy demands, which could lead to altered mitochondrial dynamics in each MSN subtype. However, there is no information into mitochondrial changes or energy homeostasis, in general, in the two MSN subtypes after cocaine exposure. Previous studies show a role for mitochondrial dynamics, including Drp1 mediated fission, in synapse formation and function (Isihara et al., 2009; Li et al., 2004; Li et al., 2008). Repeated cocaine conditions result in altered synaptic plasticity, in MSN subtypes, with enhanced excitatory plasticity occurring in D1-MSNs (Bock et al., 2013; 2008; Graziane et al., 2016; Kim et al., 2011; MacAskill et al., 2014; Pascoli et al., 2014). Thus it is plausible that altered mitochondrial dynamics could underlie these characteristic cocaine-induced synaptic changes. In this study we demonstrate a new role for Drp1 mediated fission in NAc D1-MSN subtypes in behavioral and cellular plasticity during early abstinence from repeated cocaine. These findings have implications for disruption of mitochondrial fission in addiction treatment.

Results

Mitochondrial fission and fusion gene expression in NAc after chronic cocaine

We first examined mRNA of mitochondrial fission and fusion molecules, since these are key regulators of mitochondrial dynamics, in repeated cocaine conditions (Figure 1). We examined mitochondrial fission genes: dynamin-related protein 1 (Drp1), a GTPase that co-assembles on the outer mitochondrial membrane to mediate fission, and fission 1 (Fis 1), an outer mitochondrial membrane receptor that recruits Drp1 to mediate fission. We also examined mitochondrial fusion genes: Mitofusin (Mfn) 1 and 2, outer membrane GTPases which may form complexes to tether mitochondria to mediate fusion, and optic atrophy protein 1 (Opa1), a GTPase that mediates fusion between inner mitochondrial membranes (Detmer and Chan, 2007; Ferguson et al., 2011; Westermann, 2010). We observed a modest but significant increase in NAc Drp1 mRNA, 24 hours after the last cocaine exposure, in mice that received repeated cocaine (20mg/kg, seven days, *i.p*; Figure 1A) and in rats that self-administer cocaine (1mg/kg/infusion for 10 days; Figure 1B). Fis1, Mfn1, and Opa1

mRNA were unchanged in NAc in these conditions. Mfn2 was increased in NAc after cocaine self-administration but unchanged after repeated cocaine. Acute cocaine (20mg/kg, *i.p.*) followed by 90 min, 4 hour, or 24 hour abstinence did not alter Drp1 mRNA. However, Fis1 and Opa1 were altered under these conditions (Figure S1A). 30 days of abstinence from cocaine, after repeated exposure (20mg/kg, seven days, *i.p*) or self-administration (1mg/kg/infusion for 10 days), did not alter mitochondrial fission or fusion mRNAs (Figure S1B, C) nor was protein for these mRNAs altered 24 hours or 30 days after repeated cocaine (20mg/kg, seven days, *i.p*; Figure S1D, E).

We next determined if the change observed in the rodent conditions occurs in human cocaine abuse. To do this we examined fission and fusion molecules in postmortem NAc of cocaine dependent individuals (Table S1; Golden et al., 2013; Robison et al., 2013). Consistent with the rodent findings we observe a significant upregulation of Drp1 mRNA in NAc of cocaine dependents (Figure 1C). Fis1, Mfn1, Mfn2, and Opa1 mRNA were unchanged in NAc of cocaine dependents (Figure 1C). Since Drp1 was significantly increased in NAc in all cocaine conditions, we investigated this molecule further.

Examination of mitochondrial fission promoting Drp1 after repeated cocaine

Drp1 phosphorylation at serine sites can affect its ability to promote fission. Phosphorylation within the Drp1 variable domain at serine 616 can enhance Drp1 mediated fission (Cho et al., 2013; Taguchi et al., 2007). Thus, we next sought to examine Drp1 phosphorylation at this site after repeated cocaine (20mg/kg, seven days, *i.p.*) or saline, in NAc tissue collected 24 hours or 30 days after the last cocaine injection. We observed a significant increase in p-Ser616-Drp1 in NAc in the cocaine group compared to the saline group, after 24 hours of abstinence (Figure 2A). p-Ser616-Drp1 returned to control conditions 30 days after the last exposure to cocaine (Figure S1E.) These data implicate increased mitochondrial fission in NAc after short abstinence from repeated cocaine exposure.

Blockade of fission promoting Drp1 during cocaine-mediated behaviors and effects on NAc neuron subtypes

Since the fission promoting p-Ser616-Drp1 was increased in NAc after cocaine exposure we next investigated whether inhibiting fission alters behavioral responses to cocaine. We used the small molecule, Mdivi-1 (Tanaka and Youle, 2008); which has been shown to block fission through preventing Drp1 self-assembly, inhibiting p-Ser616-Drp1, and blocking GTPase activity of the yeast Drp1 homolog (Cassidy-Stone et al., 2008; Chen et al., 2016; Kim et al., 2016). Mice received Mdivi-1, systemically or via intra-NAc infusions, during cocaine conditioned place preference (CPP), cocaine locomotor sensitization, and cocaine self-administration. For the CPP study, mice received Mdivi-1 (12.5mg/kg, 25mg/kg, or 50mg/kg; *i.p.*) or vehicle during the cocaine (7.5mg/kg) conditioning and vehicle during the saline conditioning. On the test day, mice that received Mdivi-1 (25mg/kg and 50mg/kg) displayed blunted time spent in the cocaine-paired chamber (Figure 2B, S2A), while not affecting locomotor behavior during the test (Figure S2B). Mdivi-1 dosing did not alter place preference or locomotor behavior in saline control conditions (Figure S2C, S2D). A low dose of cocaine (4mg/kg) did not alter place preference in vehicle or Mdivi-1 groups (Figure S2E, F). Intra-NAc infusion of Mdivi-1 (800μM) during cocaine conditioning

blunted place preference (Figure 2C, S2G) but did not alter locomotor behavior during the test day (Figure S2H). Similar to previous studies (Chen et al., 2016; Kim et al., 2016), Mdivi-1 (50mg/kg) blocked the p-Ser16-Drp1 induction in NAc 24 hours after repeated cocaine (20 mg/kg, 7 days, *i.p.*; Figure S2K) and Mdivi-1 treatment. Mdivi-1 did not alter mRNA or protein for total Drp1 or other fission or fusion molecules (Figure S2K and M). Nor did it alter these molecules or p-Ser616-Drp1 30 days after cocaine and Mdivi-1 exposure (Figure S2L and N).

To determine if Mdivi-1 can also alter cocaine-induced locomotor responses, mice were given Mdivi-1 (25mg/kg or 50mg/kg) during seven days of cocaine (10mg/kg) locomotor sensitization. Mdivi-1 did not alter locomotor responses, compared to vehicle controls, during this acquisition phase (Figure 2D). However, during a cocaine (10mg/kg) challenge injection, after seven days of abstinence, mice that received 50mg/kg Mdivi-1 during the acquisition phase displayed blunted expression of cocaine locomotor sensitization (Figure 2D, S2I). Mdivi-1 did not alter locomotor responses when paired with saline injections (Figure S2J).

We next sought to examine if the effects of Mdivi-1 occurred through a specific NAc MSN subtype since these two subtypes, D1-MSNs vs. D2-MSN, in NAc and dorsal striatum, display distinct cellular and molecular plasticity roles to cocaine (Bock et al., 2013; Chandra et al., 2015; Heiman et al., 2008; Kim et al., 2011; Lobo et al., 2010; Lobo et al., 2013; MacAskill et al., 2014; Pascoli et al., 2014; Graziane et al., 2016; Calipari et al., 2016; Creed et al., 2016), We examined c-Fos protein (a marker for neuronal activity) in D1-tdTomato mice 90 minutes after a cocaine (20mg/kg, *i.p.*) challenge in mice that were abstinent (7 days) from repeated cocaine (20mg/kg, 7 days, *i.p.*) or saline, along with vehicle or Mdivi-1 (50mg/kg) treatment (Figure 3A). c-Fos was significantly increased in D1-tdTomato positive neurons (D1-MSNs) but unchanged in D1-tdTomato negative neurons (mainly D2-MSNs), in the cocaine-vehicle group compared to saline-vehicle controls. The Mdivi-1- cocaine group displayed blunted c-Fos induction in D1-MSNs, which was similar to saline controls (Figure 3B). Interestingly, the D1-tdTomato negative neurons had a slight increase in c-Fos in the Mdivi-1- cocaine group, compared to saline controls, but this was unchanged compared to the vehicle-cocaine group (Figure 3B). Since Mdivi-1 blocked the characteristic cocaine-mediated c-Fos induction in D1-MSNs, we next examined whether excitatory synaptic function was altered in this MSN subtype. We recorded from D1-MSNs 24 hours after the last dose of cocaine following repeated cocaine (20mg/kg, 7 days, *i.p.*) and Mdivi-1 (50mg/kg) exposure (Figure 3C). Mdivi-1 blocked the potentiated AMPA/NMDA ratio and AMPA current rectification index, observed in D1-MSNs, after repeated cocaine exposure (Figure 3C, 3D). However, under these same conditions, Mdivi-1 did not alter basic membrane properties in D1-MSNs (Figure S3A–F).

Ribosome-associated Drp1 mRNA and activated Drp1 protein in NAc MSN subtypes after repeated cocaine

Since the effects of Mdivi-1 during cocaine exposure blunt c-Fos induction and excitatory synaptic properties in D1-MSNs, we next investigated if the increase in NAc Drp1 was occurring in these MSN subtypes after repeated cocaine. We first examined Drp1 mRNA in

NAc MSN subtypes after repeated cocaine. To do this we used RiboTag (RT) mice, which have a Cre-inducible hemagglutinin (HA) tagged ribosomal protein L22 (Rpl22), that were crossed to D1-Cre or D2-Cre mice (Chandra et al., 2015; Gerfen et al., 2013; Gong et al., 2007; Sanz et al., 2009). This allows isolation of D1-MSN and D2-MSN ribosomes and subsequent purification of MSN subtype ribosome-associated mRNA (actively translating mRNA; Figure 4A). We previously demonstrated enrichment of D1-MSN and D2-MSN marker genes in their respective neuron populations using this approach (Chandra et al., 2015). Ribosome-associated mRNA was isolated from NAc of D1-Cre-RT and D2-Cre-RT mice that received i.p. injections of cocaine (20mg/kg) or saline for seven days, followed by 24-hour withdrawal (Figure 4B). Drp1 translating mRNA was significantly upregulated in NAc D1-MSNs after cocaine exposure (Figure 4B). In contrast, cocaine exposure resulted in a downregulation of Drp1 translating mRNA in NAc D2-MSNs (Figure 4B). Fis1, Mfn1, Mfn2, and Opa1 mRNA were unaltered in either MSN subtype after repeated cocaine, although, we did observe a trend in increased Mfn1 mRNA in D2-MSNs (Figure S4A, B). Additionally, these genes displayed no difference in enrichment of fission and fusion gene mRNAs, in MSN subtypes, in cocaine naïve conditions (Figure S4C). We next examined the fission promoting p-Ser616-Drp1 protein colocalization in D1-MSNs and D2-MSNs after repeated cocaine (20mg/kg, 7 days, *i.p.*; Figure 4C). We observed a significant increase in p-Ser16-Drp1 in D1-MSNs and a decrease in D2-MSNs after repeated cocaine (Figure 4D).

Mitochondrial dynamics in NAc MSN subtypes after cocaine self administration

We sought to determine if the increase in translating Drp1 mRNA and active Drp1 protein in D1-MSNs, after repeated cocaine, indicates altered mitochondrial dynamics in these neurons. We examined this in D1-Cre mice that underwent 10 days of intravenous cocaine (0.5mg/kg/infusion, FR1 schedule) or saline self-administration, followed by a 24-hour abstinence period (Figure 5A). We developed a Cre-inducible double inverted open (DIO) reading frame adeno-associated virus (AAV) expressing mito-dsRed (Sterky et al., 2011) to label mitochondria in MSN subtypes (Figure S5A). This approach allows quantification of mitochondrial volume, density, and size. D1-Cre mice received NAc injections of AAV-DIO-mito-dsRed and a Cre-inducible AAV to label MSN cell bodies with EYFP (Figure 5C) followed by cocaine or saline self-administration (Figure 5A, B).

Given that the dendritic arbor in MSNs comprises a large part of the cytosol (Wilson et al., 1983) and since Drp1 is implicated in dendritic plasticity (Li et al., 2004), we examined mitochondria in D1-MSN dendrites after cocaine self-administration. We examine mitochondria in proximal dendrites, within 50μm radius from soma; distal dendrites, >100μm radius from the soma; and distal secondary dendrites, the first nearest branch from the distal dendrite. Cocaine self-administration led to an increase in the frequency of smaller length mitochondria in D1-MSN dendrites. Mitochondria with <1.5μm length were increased in proximal dendrites, while mitochondria with 1.5μm-3μm length were increased in distal dendrites and distal secondary dendrites in the cocaine group compared to saline controls (Figure 5E). Additionally, cumulative frequency distribution plots suggest reduction in larger length mitochondria and demonstrate a leftward shift toward smaller length mitochondria in all D1-MSN dendrites in mice that self-administer cocaine (Figure 5F). Consistent with these data, we observed a reduction in overall mitochondrial length in D1-

MSN dendrites in the cocaine group (Figure 5F). We also examined mitochondria in D2-MSNs after cocaine self-administration but observed only a reduction in the frequency of smaller mitochondria (1.5–3μm) and an increase in larger mitochondria (3–4.5μm) in the distal secondary dendrites of these MSNs after cocaine-self administration. Overall mitochondrial length in D2-MSN dendrites was unaltered in the cocaine group compared to saline controls (Figure S5B-F). Mitochondrial density (per dendrite 10μm length) was increased, while mitochondrial index (mitochondrial length per 10μm dendrite length) was reduced in proximal D1-MSN dendrites in the cocaine group (Figure S5G). Mitochondrial density and index were unchanged in D2-MSN dendrites after cocaine self-administration (Figure S5J-L). Mitochondrial volume (per volume dendrite) was unaltered in dendrites of either MSN subtype after cocaine self-administration (Figure S5G-I and S5J-L). These results collectively suggest increased mitochondrial fission occurs in D1-MSN dendrites after cocaine self-administration. This is consistent with increased active Drp1, in NAc D1-MSNs, after cocaine exposure (Figure 4). The results are also consistent with reduction of p-Ser616-Drp1, by Mdivi-1, resulting in blunted c-Fos activity and blunted excitatory synaptic function in D1-MSNs (Figure 3, S2). Consistent with these data, Mdivi-1 (50mg/kg) exposure prevented the repeated cocaine (20mg/kg, 7 days, i.p.) mediated induction of smaller mitochondria in D1-MSNs (Figure S5M-N).

Viral mediated Drp1 knockdown or fission promoting Drp1 enhancement in D1-MSNs during cocaine self administration and cocaine seeking

Since our data implicate enhanced fission, through Drp1 in D1-MSNs, after cocaine exposure and Mdivi-1 prevents cocaine-induced fission in D1-MSN dendrites, while also blocking behavioral responses to cocaine; we sought to directly reduce Drp1 levels in D1-MSNs. We generated a Cre-inducible AAV-DIO-Drp1-miRNA(miR)-mCitrine, designed from an shRNA, and a AAV-DIO-scramble sequence (SS)miR-mCitrine control (Figure S6A). We use this miR approach similar to previous studies that achieve mRNA and protein knockdown in the brain, as well as demonstrate gene specific knockdown (Chandra et al., 2015, 2017; Damez-Werno et al., 2016; Francis et al., 2017; Maze et al., 2015; Sun et al., 2015). AAVs were injected into the NAc of D1-Cre mice and expression was visualized with mCitrine fluorescence (Figure 6A, S6B). D1-Cre NAc expressing DIO-Drp1-miR displayed decreased Drp1 mRNA, total Drp1 and p-Ser616-Drp1 (Figure 6B, C, D). After viral infusion mice underwent water training followed by intravenous catheter surgeries and subsequently underwent 10 days of cocaine (0.5mg/kg/infusion, FR1 schedule) self-administration (Figure 6E). Drp1-miR knockdown in D1-MSNs did not alter acquisition to cocaine self-administration (Figure 6F). Twenty-four hours after the last cocaine self-administration D1-Cre mice were placed back in the chamber to test seeking for cocaine (Lee et al., 2013; Li et al., 2015; Sun et al., 2016; Werner et al., 2015), and the Drp1-miR group displayed a significant reduction in cocaine seeking (Figure 6G). Drp1-miR knockdown in D1-MSNs did not alter reinforcement for a natural reward (Figure S6C). Examination of mitochondria size demonstrated an increase in larger mitochondria in D1-MSN dendrites in the Drp1-miR group compared to SS-miR controls (Figure 6H, I), implicating reduced fission in D1-MSN dendrites with Drp1 knockdown. Further, Drp1-miR in D1-MSNs blunted c-Fos induction in these neurons when given a challenge cocaine injection after repeated cocaine (10 days, 20mg/kg; Figure 6J, K). We observed no

significant difference in c-Fos colocalization in D1-MSNs in the Drp1-miR group receiving cocaine compared to SS-miR group receiving saline injections (Figure 6K).

We next directly tested whether enhancing fission in D1-MSNs can modify behavioral responses to cocaine. We expressed the fission promoting Drp1(S637A) mutant, or wildtype (WT) Drp1 in D1-MSNs and examined cocaine self-administration behaviors. The ability of Drp1(S637A) to enhance fission occurs via a mutation at the serine 637 fission repressing phosphorylation site on the GTPase effector domain, which prevents phosphorylation at this site (Cereghetti et al., 2008; Chang and Blackstone, 2007). We generated Cre-inducible DIO-AAVs to overexpress Drp1(WT)-EYFP or a Drp1(S637A)-EYFP (Figure S7A). D1-Cre mice received infusions of AAV-DIO-Drp1(WT)-EYFP, AAV-DIO-Drp1(S637A)-EYFP, or control virus AAV-DIO-EYFP into the NAc. AAV expression was visualized with EYFP fluorescence (Figure 7A, S7F). Drp1 mRNA was significantly increased in NAc of D1-Cre mice that received Drp1(WT) and Drp1(S637A) AAVs compared to EYFP controls (Figure 7B). Drp1(S637A) overexpression resulted in expression of the fission promoting p-Ser616-Drp1-EYFP fusion protein in NAc (Figure 7C). After viral infusion D1-Cre mice underwent water training, followed by intravenous catheter surgeries, and subsequently underwent 10 days of cocaine (0.5mg/kg/infusion, FR1 schedule) self-administration (Figure 7D). Expression of Drp1(S637A) in D1-MSNs enhanced acquisition to self-administration on day one compared to EYFP controls, and on day seven compared to Drp1(WT) conditions (Figure 7E). Twenty-four hours after the last cocaine self-administration D1-Cre mice were placed back in the chamber to test seeking for cocaine (Lee et al., 2013; Li et al., 2015; Sun et al., 2016; Werner et al., 2015). We observed no difference in seeking between the three virus conditions in D1-Cre mice at this time point (Figure S7D). However, Drp1(S637A) expression in D1-MSNs resulted in increased seeking for cocaine after 30 days of abstinence compared to Drp1(WT) and EYFP conditions (Figure 7F). Drp1(S637A) and Drp1(WT) expression in D2-Cre NAc did not alter cocaine self-administration or seeking behavior (Figure S7B, C, E). Additionally, Drp1(S637A) and Drp1(WT) expression in either MSN subtype did not alter reinforcement for a natural reward (Figure S7D). Examination of mitochondrial size demonstrated enhanced frequency of smaller mitochondria (<1.5μm) and a reduction in larger mitochondria (3–4.5μm) in D1-MSN dendrites of the Drp1(S637A) group (Figure 7G, H). At this 30 day abstinent time point fission was no longer increased in D1-MSNs of mice that self-administered cocaine compared to saline (Figure S7H). Our data implicate that enhancing the fission promoting Drp1 variant, thus enhancing fission, increases drug seeking after prolonged abstinence from cocaine self administration. Finally, examination of c-Fos, after a challenge cocaine injection, in mice that were abstinent from repeated cocaine (20mg/kg, 10 days) for 30 days demonstrated enhanced c-Fos colocalization in D1-MSNs expressing Drp1(S637A) compared to Drp1(WT) or EYFP, as well as and EYFP group receiving saline injections (Figure 7I, J). EYFP and Drp1(WT) cocaine conditions also displayed increased c-Fos induction compared to saline controls (Figure 7I).

Discussion

Our study establishes a direct role of altered mitochondrial dynamics, specifically altered mitochondrial fission, in D1-MSN subtypes during the early abstinence from cocaine

(Figure 8). Previous studies indicate altered mitochondrial function in the brain after cocaine exposure (Cunha-Oliveira et al., 2013; Dietrich et al., 2005; Feng et al., 2014; Jang et al., 2015; Lehrmann et al., 2003; Pomierny-Chamiolo et al., 2013). However, there has been no investigation into cocaine mediated mitochondrial dynamics, and the molecular mediators of these mitochondrial processes, in the brain. We demonstrate for the first time altered mitochondrial dynamics with repeated cocaine exposure.

Rodents exposed to repeated cocaine, investigator administrated and self administered, have increased Drp1 mRNA in NAc. This finding translates to human addiction since cocaine dependent individuals display increased NAc Drp1 mRNA. Further, the phosphorylated Ser616 Drp1, which mediates fission (Cho et al., 2013; Taguchi et al., 2007), is increased in NAc after repeated cocaine. Interestingly total Drp1 levels are not increased in NAc, but this could reflect the masking of an increase in D1-MSNs when collecting total NAc tissue; which includes both of the MSN subtypes, interneurons, and non-neuronal cells. The lack of change in total Drp1 may reflect a differential change occurring across many cell populations. Whereas, the increase observed in p-Ser616-Drp1 could reflect a more specific increase occurring in D1-MSNs, since we detect increased colocalization of p-Ser616-Drp1 in these MSNs after repeated cocaine. Further, our observation that translating Drp1 mRNA is increased in NAc D1-MSNs after repeated cocaine suggests an increase in total protein in these neurons. Blockade of fission either systemically or intra-NAc, with Mdivi-1 (Tanaka and Youle, 2008; Cassidy-Stone et al., 2008; Chen et al., 2016; Kim et al., 2016), blunts place preference for cocaine, blocks the expression of cocaine-induced locomotor sensitization, and blunts seeking behavior after cocaine self-administration. The ability of Mdivi-1 to blunt these cocaine-induced behaviors implicates therapeutic potential of Mdivi-1 in cocaine addiction.

Examination into MSN subtypes demonstrates blunted cocaine-induced c-Fos expression in D1-MSNs with Mdivi-1 treatment. We also observed attenuated AMPA/NMDA and AMPA current rectification index in D1-MSNs, with Mdivi-1 treatment, during repeated cocaine. These data implicate reduced activity and excitatory synaptic function in D1-MSNs when blocking Mdivi-1 during cocaine exposure. Our data showing that Mdivi-1 blunts cocaine-induced p-Ser616-Drp1 in NAc and prevents cocaine-induced smaller mitochondria in D1-MSNs, suggests that the blunted cocaine-mediated behavioral and plasticity effects, with Mdivi-1, occur through blockade of Drp1 mediated fission. This is consistent with previous studies demonstrating Mdivi-1 blocks mitochondrial fission through reducing p-Ser616-Drp1 and reducing GTPase activity in the yeast Drp1 homolog (Cassidy-Stone et al., 2008; Chen et al., 2016; Kim et al., 2016). However, a recent study calls into question the role of Mdivi-1 as a select Drp1 inhibitor. This study showed that Mdivi-1 is a reversible mitochondrial complex I inhibitor that modulates reactive oxygen species (ROS), without altering mitochondrial elongation or causing Drp1 GTPase activity impairment (Bordt et al., 2017). Thus, we cannot rule out that the behavioral and plasticity effects of Mdivi-1 are occurring through other mechanisms, such as reducing ROS production. Nonetheless, our data demonstrating reduced p-Ser616-Drp1 and reduced smaller mitochondria in D1-MSNs, with Midivi-1 exposure, suggests that Mdivi-1 may directly or indirectly inhibit Drp1 mediated fission in D1-MSNs to reduce the behavioral and plasticity adaptations occurring with repeated cocaine. Finally, one cannot rule out differential effects of Mdivi-1 based on

the experimental condition, *in vitro* cell culture application and analysis (Bordt et al., 2017) vs. intra-brain or systemic application with *in vivo* brain analysis, the latter condition reflecting our current study.

The D1-MSN subtype response to Mdivi-1 is consistent with increased levels of translating Drp1 mRNA and fission promoting Drp1 protein, in D1-MSNs, after repeated cocaine. Consistent with these findings, we observe alterations in mitochondrial dynamics in D1-MSN dendrites after cocaine self-administration, which are indicative of increased mitochondrial fission (Detmer and Chan, 2007; Friedman and Nunnari, 2014; Westermann, 2010). The increased D1-MSN dendritic fission and enhanced excitatory synaptic function are in line with Drp1 mediating dendritic plasticity and synapse formation (Ishihara et al., 2009; Li et al., 2004). These results are also consistent with enhanced plasticity occurring in D1-MSNs, as well as induction of molecules mediating plasticity in D1-MSNs after chronic cocaine, after repeated cocaine exposure (Chandra et al., 2015; Grueter et al., 2013; Kim et al., 2011; Lobo et al., 2013; MacAskill et al., 2014; Pascoli et al., 2014).

Our findings suggest that fission in D1-MSNs may be involved in motivational aspects of cocaine. Indeed, we demonstrate that viral mediated D1-MSN specific knockdown of Drp1 in D1-MSNs, blunts drug seeking after early abstinence from cocaine self-administration, while also blunting c-Fos induction and fission in D1-MSNs. Viral mediated expression of a fission promoting Drp1(S637A) variant (Cereghetti et al., 2008; Chang and Blackstone, 2007), selectively in D1-MSNs, enhances cocaine seeking after long-term abstinence, while increasing fission in D1-MSNs at this time point. Interestingly, Drp1(S637A) expression in D1-MSNs did not enhance cocaine seeking 24 hours after the last self-administration session. This could reflect the inability to promote fission further in these MSNs at this time point. Whereas, during the 30 day abstinent period, fission returns to basal levels in mice that self-administer cocaine; thus enhancing fission at this time point led to increased cocaine seeking. Finally, we were surprised that the Drp1(WT) expression in D1-MSNs did not enhance cocaine seeking, since previous *in vitro* studies show that Drp1(WT) expression can enhance fission and structural plasticity in hippocampal neuronal cultures (Li et al., 2004). Consistent with the lack of behavioral outcome with Drp1(WT), we do not observe enhanced fission in D1-MSN dendrites in the Drp1(WT) compared to EYFP virus controls. It is plausible that a threshold for Drp1 activation occurs after multiple drug episodes, which could be a consequence of upstream kinases, or other mechanisms. Thus enhanced Drp1 levels may not be sufficient to enhance active Drp1 and corresponding mitochondrial changes in the presence of cocaine.

Our studies contribute to the emerging role for mitochondrial adaptations in diseased motivational states including mood disorders, stress, and addiction (van der Kooij et al., 2017; Cai et al., 2015; CONVERGE consortium, 2015; Cunha-Oliveira et al., 2013; Dietrich et al., 2005; Feng et al., 2014; Hollis et al., 2015; Jang et al., 2015; Lehrmann et al., 2003; Manji et al., 2012; Picard et al., 2015; Pomierny-Chamiolo et al., 2013). We demonstrate a novel role of altered mitochondrial dynamics in D1-MSN subtypes in cocaine abuse; which occurs during early abstinent time points (Figure 8). These studies have direct implication for pharmacological therapeutics with agents that target mitochondrial dynamics for treatment of psychostimulant addiction.

STAR Methods

CONTACT FOR REAGENTS AND RESOURCE SHARING

Further information and requests for resources and reagents should be directed to and will be fulfilled by the Lead Contact, Mary Kay Lobo (mklobo@som.umaryland.edu).

EXPERIMENTAL MODEL AND SUBJECT DETAILS

Animal studies—All studies were conducted in accordance with the guidelines set up by the Institutional Animal Care and Use Committee's at The University of Maryland School of Medicine and The University at Buffalo, The State University of New York. In both institutions, animals' health status was closely monitored by the veterinary staff and the experimenters throughout the experiments. D1-Cre hemizygote (line FK150) or D2-Cre hemizygote (line ER44) bacterial artificial chromosome (BAC) transgenic mice from GENSAT (Gong et al., 2007, Gerfen et al., 2013) (www.gensat.org) on a C57BL/6J background were used for mitochondrial counting and Drp1 virus behavioral experiments. Homozygous RiboTag (RT) mice on a C57BL/6J background, expressing a Cre-inducible HA-Rpl22 (Sanz et al., 2009) were crossed to D1-Cre or D2-Cre mouse lines to generate D1-Cre-RT and D2-Cre-RT mice (Chandra et al., 2015) and used for cell type–specific ribosome-associated mRNA isolation. C57BL/6J mice obtained from Jackson Laboratory were used for RT-PCR, western blot, and behavioral experiments. For c-Fos immunostaining experiments, D1-tdTomato BAC mice (Shuen et al., 2008) on a C57BL/6J background were obtained from Jackson Laboratory. Male mice, 8 week-old at the beginning of the experiments, have been used for this study. All mice were naïve to any previous experiment and were maintained on a 12h light/dark cycle *ad libitum* food and water. Mice were group housed (3–5 per cage) for all experiments. For self-administration studies, mice were housed 2 per cage across a perforated divider to allow sensory contact. Naïve male Sprague-Dawley rats (250–275g at the beginning of the experiment), used for self-administration cDNA, were maintained on a 12h reverse light/dark cycle *ad libitum* food and water. After catheterization surgery, rats were single housed for the duration of the experiments. For all *in vivo* studies, animals were randomly assigned to the treatment or control group.

Human post-mortem tissue—The cohort was composed of 24 males and 2 female, ranging in age between 20 and 53 years. All subjects died suddenly without a prolonged agonal state or protracted medical illness. In each case, the cause of death was ascertained by the Quebec Coroner Office, and a toxicological screen was conducted with tissue samples to obtain information on medication and illicit substance use at the time of death. The subject group consisted of 14 individuals who met the Structured Clinical Interview for DSM-IV (Diagnostic and Statistical Manual of Mental Disorders-IV) Axis I Disorders: Clinician Version (SCID-I) criteria for cocaine dependence. The control group comprised 12 subjects with no history of cocaine dependence and no major psychiatric diagnoses. The processing of the tissue is described elsewhere (Golden et al., 2013; Robinson et al., 2013). Briefly, hemispheres were immediately separated by a sagittal cut into 1-cm-thick slices and placed in a mixture of dry ice and isopentane (1:1 (vol:vol). The frozen tissue was then stored at −80°C. The list of individual samples is described in Table S1.

Cell line—Male Neuro-2a cell line was purchased form Sigma (Cat# 89121404) and maintained at 37°C, 5% CO2 in DMEM with GlutaMAXI, 4500 mg/L glucose and 110 mg/L sodium pyruvate (Invitrogen) supplemented with 10% v/v FCS (Invitrogen) as described in Chandra et al., 2015. Cells were routinely tested for mycoplasma contamination.

METHOD DETAILS

Experimental design—For all experiments, sample size was based on animal number used in our previous studies (Chandra et al., 2013, 2015, Chandra et al., 2016, Lobo et al., 2010, 2013, Gancarz et al. 2015). Animals were randomly assigned to experimental groups by cage before surgery and/or treatment. Further, the order of the animals was randomized before behavioral tests. For all behavioral tests, data quantification (time, distance, number of infusions, nosepokes) was objectified by the use of dedicated software (CleverSys, MED-PC). For mitochondrial quantification, the experimenter was blind to the treatment conditions. Animals with bad viral expression (absent or off-target) or cannula placement as well as loss of catheter patency were excluded from the analysis. Grubbs outlier test was performed on data with obvious outliers and no more than one animal or sample was removed per group.

Repeated cocaine treatment—C57BL/6J, D1-Cre-RT, and D2-Cre-RT mice received 7 daily intraperitoneal injections (i.p.) of cocaine (20mg/kg) or 0.9% saline in the home cage. NAc tissue was collected 24h after the last injection. Cocaine hydrochloride (Sigma) was dissolved in sterile saline. The dose of cocaine was selected based on previous studies (Chandra et al., 2013, 2015, Lobo et al., 2010, 2013).

Conditioned place preference—Conditioned place preference (CPP) was conducted as previously described using Topscan tracking software (CleverSys) (Chandra et al., 2013; Lobo et al., 2010) Briefly, the conditioning chambers consisted of two distinct environments with unique wall patterns and floor textures separated by a neutral chamber. On the first day, mice were allowed to freely explore the 3 chambers for 20 min. Groups were then balanced and adjusted for any chamber bias that may have occurred (mice that showed significant preference for one compartment were excluded from the experiment). During the conditioning days 2 and 3, mice received an i.p. injection of saline before noon and were confined for 30 min to one chamber. In the afternoon, mice received an injection of Mdivi-1 (12.5mg/kg, 25mg/kg, or 50mg/kg in corn oil, ip) or vehicle 1 hour prior to receiving a cocaine injection (7.5mg/kg in saline, ip) and were placed in the chamber, opposite to the saline conditioning for 30 min. On day 4, animals were placed in the apparatus for 20 min without any treatment. Time spent in the drug-paired chamber before and after conditioning were compared as well as time spent in the drug-paired chamber minus time spent in the saline-paired chamber. To test the potential aversive effect of Mdivi-1 on CPP, a dose of 4mg/kg (in saline, ip) was used (Dietz et al., 2012). For Mdivi-1 infusion experiments, mice were implanted with cannula (Plastics One) into the NAc 4 days before the experiment. On the two conditioning days, mice were microinjected with 800μM/0.5μL/hemisphere of Mdivi-1 (in 35% DMSO in saline) or vehicle immediately prior to each cocaine pairing session. On the last day, mice were tested without any microinjection.

Cocaine-induced locomotion—Cocaine-induced locomotor activity was performed using protocols routinely used in our laboratory (Chandra et al., 2013, 2015; Lobo et al., 2010). Briefly, C57/Bl6 mice were habituated to the apparatus for 30 min. On the next day, basal locomotion was recorded for 30 min after one saline injection. Mice received a daily injection (for seven days) of Mdivi-1 (25 mg/kg or 50mg/kg in corn oil, ip) or vehicle 1 hour prior to receiving a cocaine injection (10mg/kg in saline, ip) or a saline injection. The Mdivi-1 doses were based on previous studies (Brooks et al., 2009; Park et al., 2011). Mice were placed in the chamber for 30 min and activity was tracked with Topscan tracking software (Clever sys). After seven days of withdrawal mice received a cocaine (10mg/kg) challenge and activity was measured for 30 min in the open field.

Intravenous cocaine self-administration—Drug self-administration procedure was adapted from our previously published studies (Chandra et al., 2013, 2015; Gancarz et al., 2015). Operant chambers (MED Associates) had two nosepoke holes on one wall and a house-light on the middle of the opposite wall. After habituation (30 min) to the operant boxes, mice were water deprived overnight. Eight training sessions of 30 min (4 days, 2 sessions/day) were performed. Active responses, under a fixed ratio 1 (FR1) schedule, elicited the delivery of a 10μL water drop associated with a light-cue both delivered in the nosepoke hole. Reward delivery was followed by a 10 sec time-out period and the house-light was turned off during this time. Inactive responses were also recorded (MED-PC software). After water training, mice were anesthetized with Ketamine (100mg/kg) and Xylazine (16mg/kg) and implanted with chronic indwelling jugular catheters (Plastics One). Animals were flushed daily with 0.1mL of a mixture of 2.27% Baytril (20%) and Heparin 50IU/mL (40%, in saline). After 5 days of recovery, mice were underwent 10 days of cocaine self-administration. Each session lasted 2 hours and was an FR1 schedule similar to the water training with the exception that each response in the active nosepoke elicited the delivery of intravenous cocaine hydrochloride (0.5mg/kg/infusion in saline). At the end of the cocaine self-administration experiment, catheter patency was tested with a 30μL intravenous infusion of ketamine (50mg/kg, in saline). Only mice that showed patency were used in data analyses. Mice then underwent seeking tests 24 hours and 30 days after the last self-administration. The seeking test was performed under extinction conditions in which a response resulted in presentation of the cue but no drug was delivered (Lee et al., 2013; Li et al., 2015; Sun et al., 2016; Werner et al., 2015). For cocaine self-administration experiment in rats, similar procedure was used. One week after catheterization, rats underwent 2 hours sessions of intravenous cocaine (or saline) self-administration (1 mg/kg/infusion in saline) under a FR1 schedule of reinforcement followed by a 30 sec time-out period for 10 days. For Mdivi-1 infusion experiments, rats were implanted with cannula (Plastics One) into the nucleus accumbens on the same day as catheterization surgery. On the last three days of FR1 cocaine self-administration, rats were microinjected with 800μM/1μL/hemisphere of Mdivi-1 (in 35% DMSO in saline) or vehicle immediately prior to each session during the last three sessions. Rats were then tested for cue-induced cocaine seeking (1 h session) on withdrawal day 1 without any microinjection prior to testing. Complete list of regents can be found in the Key resource table.

Mouse stereotaxic surgery—D1-Cre or D2-Cre mice were anesthetized using 4% isoflurane in a small induction chamber. After the initial induction, isoflurane was maintained at 1% for the remainder of the surgery. Animals were placed in a stereotaxic instrument and their skull was exposed. 33 gauge Hamilton syringe needles were used to inject 0.6μl of either AAV-DIO-EYFP, AAV-DIO-Drp1(WT)-EYFP, AAV-DIO-Drp1(S637A), AAV-DIO-Drp1-miR, AAV-DIO-scramble-miR or 0.2ul of AAV-DIO-mito-dsRed with AAV-DIO-ChR2-EYFP bilaterally into the NAc (anterior/posterior, AP+1.6; medial/lateral, ML±1.5; dorsal/ventral, DV−4.4, 10° angle) according to our previous studies (Chandra et al., 2015; Lobo et al., 2010). Mice were then returned to the vivarium for 2 weeks to allow for recovery and maximal virus expression.

Slice Physiology—Twenty four hours following the final cocaine and Mdivi-1 or vehicle treatment, male *Drd1a*-tdTomato mice were euthanized and coronal mouse brain slices, 220 μm in thickness were prepared in cooled artificial cerebrospinal fluid containing (in mM): NaCl 119, KCl 2.5, MgCl 1.3, CaCl2 2.5, Na2HPO4 1.0, NaHCO3 26.2 and glucose 11, bubbled with 95% O2 and 5% CO2. Slices were kept at 32- 34°C in a recording chamber superfused with 2.5 ml/min artificial cerebrospinal fluid. Visualized whole-cell voltage-clamp recording techniques were used to measure holding and synaptic responses of D1-MSNs of the NAc, identified by the presence of the td-Tomato of BAC transgenic mice by using a fluorescent Nikon 600 microscope, as described previously (Creed et al., 2016; Patton et al., 2016). Holding potential was maintained at −70 mV for AMPA/NMDA ratio experiments and at −60 mV for membrane properties assessment using a Multiclamp 700B amplifier (Molecular Devices). Access resistance was monitored by a depolarizing step of −14 mV each sweep, every 10 s. Experiments were discarded if the access resistance varied by more than 10%. For AMPA/NMDA ratio, currents were amplified, filtered at 5 kHz and digitized at 20 kHz and for membrane properties at 2 kHz, digitized at 10 kHz. Both were acquired using Clampex v10.4 software (Molecular Devices). All experiments were performed in the presence of picrotoxin (100 μM) to isolate excitatory transmission. Internal solution contained (in mM) 130 CsCl, 4 NaCl, 5 creatine phosphate, 2 MgCl2, 2 Na2ATP, 0.6 Na3 GTP, 1.1 EGTA, 5 HEPES and 0.1 mm spermine. Synaptic currents were electrically evoked by stimuli (50 μs) at 0.1Hz through bipolar stainless steel electrode placed onto the tissue. To isolate AMPAR-evoked EPSCs, the NMDA antagonist D-AP5 (50 μM) was bath applied. The NMDAR component was calculated as the difference between the EPSCs measured in the absence and presence of D-AP5. The AMPAR/NMDAR ratio was calculated by dividing the peak amplitudes. The rectification index of AMPAR-mediated currents was calculated as the ratio of the chord conductance calculated at −70 mV, divided by chord conductance at +40 mV. In sample traces, stimulation artifacts were removed.

For membrane properties, capacitance, membrane and input resistances, resting membrane potential, action potential threshold and the maximum firing rate of D1-expressing MSNs were made in current clamp mode using recording pipettes of 2.5–5 MΩ resistance (Sutter Instruments) filled with a potassium-based internal pipette solution (in mM: 126 potassium gluconate, 4 KCl, 10 HEPES, 4 ATP-Mg, 0.3 GTP-Na and 10 phosphocreatine, osmolarity: 290–300, pH: 7.3). Input resistance was calculated by delivering a series of hyperpolarizing

current steps to MSNs (−150 pA for approximately 4 seconds) and measuring the voltage deflection. To calculate the action potential threshold, a ramp of depolarizing current was delivered to cells in current clamp mode and the voltage at which an action potential detonated was recorded. The maximum firing rate of these neurons was determined by delivering increasing depolarizing current steps and calculating the maximum frequency at which the cells could fire faithfully.

Adeno-Associated Viral Vectors—Recombinant Cre-dependent adeno-associated viruses (AAVs) mito-dsRed, ChR2-EYFP, Drp1(WT) and Drp1(S637A) were used in this study. The mito-dsRed (Sterky et al., 2011) and Drp1(WT) or Drp1(S637A) (Labrousse et al., 1999; Ingerman et al., 2005) vectors were gifted from Dr. N.G. Larsson (Max Planck Institute for Biology of Ageing, Cologne, Germany) and Mariusz Karbowski (University of Maryland, Baltimore, USA) respectively. mito-dsRed, Drp1(WT), and Drp1(S637A) sequences were PCR amplified (Phusion DNA polymerase, New England Biolabs) and an EYFP tag was added to Drp1(WT), and Drp1(S637A) vector. Drp1-miR was generated from Drp1 shRNA by conversion from shRNA to miR as described in (Chandra et al., 2015). Briefly, four Drp1 shRNA expression vectors were purchased from Origene and tested in Neuro2a cells. The most efficient shRNA was chosen for miR engineering using the BLOCK-iT Pol II miR RNAi Expression Vector Kit (Invitrogen). Two single-stranded DNA oligonucleotides were designed, one encoding the target pre-miR top strand oligo and the other the bottom strand oligo compliment. Top and bottom strand oligos were annealed to generate a double-stranded oligonucleotide and cloned into a pcDNA-EmGFP-miR vector. Then, vectors were PCR cloned into the EF1a-DIO vector. The DIO-ChR2-EYFP and DIO-EYFP was used in the mitochondrial quantification studies. DIO-EYFP and DIO-scramble-mCitrine was used as control in the behavioral studies. Both vectors were packaged into AAV (serotype 2) at University of North Carolina (UNC) Vector Core Facility. Virus packaging for AAV-DIO-mito-dsRed, AAV-DIO-Drp1(WT)-EYFP and AAV-DIO-Drp1(S637A)-EYFP (serotype 2), AAV-Drp1-miR-IRES-mCitrine and AAV-Scramble sequence (SS)-miR-IRES-mCitrine was performed as described previously (Chandra et al 2015; Prasad et al., 2011). Complete list of regents can be found in the Key resource table.

Polyribosome Immunoprecipitation, RNA Isolation—Immunoprecipitation of polyribosome was prepared from NAc of D1-Cre-RT and D2-Cre-RT mice according to our previous study (Chandra et al., 2015; Chandra et al., 2016) In brief, four 14-gauge NAc punches per animal (four animals pooled per sample) were collected and homogenized by douncing in homogenization buffer and 800μl of the supernatant was added directly to the HA-coupled beads (Invitrogen: 100.03D; Covance: MMS-101R) for constant rotation overnight at 4°C. The following day, magnetic beads were washed three times in magnet for five minutes in high salt buffer. Finally, RNA was extracted by adding TRK lysis buffer to the pellet provided in MicroElute Total RNA Kit (Omega) according to manufacturer's instructions. RNA was quantified with a NanoDrop (Thermo Scientific). Complete list of regents can be found in the Key resource table. For cDNA synthesis and qRT-PCR see below.

RNA extraction and quantitative RT-PCR—Mouse and rat NAc tissue punches were collected 24 h after the last cocaine administration and stored at −80°C. RNA was extracted using Trizol (Invitrogen) and the MicroElute Total RNA Kit (Omega) with a DNase step (Qiagen). For human postmortem NAc tissue, total RNA was isolated by using Trizol (Invitrogen) as described before (Golden et al., 2013). Human RNA integrity was determined on an Agilent Bioanalyzer. All RNA quantity was measured on a Nanodrop. 300–400ng cDNA was then synthesized using reverse transcriptase iScript cDNA synthesis kit (Bio-Rad). mRNA expression changes were measured using quantitative polymerase chain reaction (qPCR) with PerfeCTa SYBR Green FastMix (Quanta). Quantification of mRNA changes was performed using the $-\Delta\Delta C_T$ method, using glyceraldehyde 3-phosphate dehydrogenase (GAPDH) as a housekeeping gene. The list of primers used in this study is included in Table S2. Complete list of regents can be found in the Key resource table.

Western blots—The NAc were homogenized in 30μl of lysis buffer containing 320mM sucrose, 5nM HEPES buffer, 1% sodium dodecyl sulfate (SDS), phosphatase inhibitor cocktails I and II (Sigma, St. Louis) and protease inhibitors (Roche) using a ultrasonic processor (Cole Parmer, Vernon Hills, IL, USA). Protein concentrations were determined using DC protein assay (Bio-Rad) and then 15–20μg samples of total protein were loaded onto Tris–HCl polyacrylamide gel (Bio-Rad). The samples were transferred to a nitrocellulose membrane and blocked for 1h in blocking buffer, 5% non-fat dry milk in Tris buffered saline (pH 7.6) with 0.1% Tween. Blocked membranes were incubated overnight at 4°C in blocking buffer with primary antibodies using either 1:1000 rabbit-anti pSer616-DRP1 (Cell Signaling, cat.# 3455S), 1:1000 DRP1 (Cell Signaling, cat.# 8570), 1:8000 GAPDH (Cell Signaling, cat.# 2118), 1:1000 OPA1 (Cell Signaling, cat.# 80471S), 1:1000 Fis1 (Santa Cruz, cat.# sc-98900), 1:1000 Mfn1 (Santa Cruz, cat.# sc-50330), 1:1000 Mfn2 (Cell Signaling, cat.# 9482). Membranes were then incubated with goat anti-rabbit peroxidase-labeled secondary antibodies (Vector Laboratories, cat.# PI-1000, 1:20,000 or 1:40,000 depending on the primary antibody used) in blocking buffer. The bands were visualized using SuperSignal West Dura Extended Duration substrate (Pierce, cat.#34075). Bands were quantified with Image Lab Software (Bio-Rad) and normalized to GAPDH to control for equal loading. Complete list of regents can be found in the Key resource table.

Immunohistochemistry—D1-Cre, D2-Cre (receiving AAV-DIO-EYFP injections into NAc) or D1-tdTomato mice were perfused with 0.1M phosphate buffered saline (PBS) followed by 4% paraformaldehyde (PFA). Brains were immersed in azide PBS overnight. Brains were dissected with a vibratome (Leica) at 100μm into 0.1M PBS for mitochondria counting or sectioned on a cryostat (Leica) at 40μm for Drp1(WT) and Drp1(S637A) virus validation and cfos counting. For pDrp1 staining, antigen retrieval was performed. Sections were placed in hot citrate buffer (10mM, pH 6) for 10 minutes. After washing with 0.1M PBS, regular immunostaing protocol was followed. Brain sections were blocked in 3% normal donkey serum with 0.3% Triton-X for 30 minutes at room temperature. Sections were then incubated overnight at room temperature in primary antibody: for pDrp1 counting, 1:1000 rabbit anti-pDrp1 (Cell Signaling cat#3455S) and 1:4000 chicken anti-GFP (Aves cat# GFP-1020), for c-Fos counting 1:8000 chicken anti-GFP (Aves cat# GFP-1020) and

1:500 Rabbit anti-c-Fos (Santa Cruz cat# sc-52) and mouse anti-NeuN (Millipore cat# MAB377) diluted in the 3% NDS and 0.3% tween 20 solution. On the second day, tissue sections were rinsed in 0.1M PBS followed by 1h incubation at room temperature in secondary antibodies, 1:1000 donkey anti-chicken-Alexa488 (Jackson ImmunoResearch cat# 703-545-155) and/or 1:1000 goat anti-rabbit Cy3 (Jackson ImmunoResearch cat# 111-166-003) and/or 1:1000 donkey anti-mouse 647 (Jackson ImmunoResearch cat# 715-605-150). Sections were rinsed in PBS, mounted onto slides, and cover-slipped. Complete list of regents can be found in the Key resource table.

Cell Counting—Cell counting was performed following protocols as described previously (Chandra et al., 2017; Lobo et al., 2013). Briefly, an Olympus Bx61 Confocal Microscope was used to image immunofluorescence. Cell counting was performed with ImageJ software (National Institutes of Health). Images sampling of NAc (from AP: 1.42 to 1.1 mm in relation to bregma) were taken from two to three brain sections/animal. A total of 250 cells were counted per brain region per mouse using 250×250 μm images. Approximately 250 total NeuN cells were counted per brain region per mouse, and then the number of D1-td-Tomato(+), D1-td-Tomato(+):c-Fos(+), D1-td-Tomato(−), and D1-td-Tomato(−):c-Fos(+) cells were counted in each region. Data were quantified by D1-td-Tomato(+):c-Fos(+) neurons × 100% / total D1-td-Tomato(+) neurons and D1-td-Tomato(−):c-Fos(+) neurons × 100% / total D1-td-Tomato(+). pDrp1 counting followed the same protocol. Approximately 250 DIO-EYFP positive cells were counted per brain region. From this population, the number of pDrp1-positive cells was counted and a percentage of colocalization was calculated: DIO-EYFP(+):pDrp1(+) × 100 / DIO-EYFP(+).

Mitochondrial Imaging—D1-Cre or D2-Cre mice were injected with AAV-mito-dsRed and co-injected with AAV-DIO-ChR2-EYFP followed by cocaine or saline self-administration. Sections were sampled from bregma AP: 1.42–1.1 mm of NAc and imaged on a Olympus Bx61 confocal microscope. A total of 8–10 cells were imaged per mouse by confocal scanning. High-resolution Z stacks images were obtained with 0.4μm increments using a 60× oil immersion objective with 2× digital zoom. Sections were scanned for neuron somas, proximal dendrites (within 50μm radius from soma), distal dendrites (over 100μm radius from the soma), and distal secondary dendrites (the first nearest branch from distal dendrite). Slides were imaged blind to the MSN subtype and drug (saline or cocaine) and mitochondria quantification was subsequently analyzed blind to both conditions.

Image analysis—Mitochondrial length, density, index, and volume was quantified using Imaris 8.2 software (Bitplane). Surface reconstruction was generated by 3D images by using the Surface tool. The background was subtracted by setting the largest diameter of images and smoothed with a Gaussian filter. Finally, 3D reconstructions of images were generated of each filter, red (mitochondria) and green (soma and dendrites). Mitochondria length was measured by using the BoundingBoxOO Length C setting that measures the length of the longest principal axis of the mitochondria. The dendrite length was determined by ‘measurement point’ tool in line pair mode. Finally, volume and length of each surface was exported by using export statistics tool. Mitochondrial volume was measured by quantifying total mitochondrial volume divided by total soma or dendrite volume. Mitochondrial density

was measured by quantifying the total number of mitochondria per 10μm length of dendrites. Dendritic mitochondrial index were measured by quantifying the average mitochondrial length per 10μm length of dendrite.

QUANTIFICATION AND STATISTICAL ANALYSIS

Graphpad Prism 6.0 software was used for statistical analysis. For ANOVA tests, Tukey post-hoc tests were used. Normal distribution was assessed by Brown-Forsythe test and similar variance between groups was tested in all groups that are statistically compared. Significance was established when p values were below 0.05. All graphs represent mean ±standard error (SEM). Sample sizes were determined from previous studies (Chandra et al., 2013, 2015, Chandra et al., 2016, Lobo et al., 2010, 2013, Gancarz et al. 2015). Grubbs outlier test was performed on data with obvious outliers and no more than one animal or sample was removed per group. Statistical tests values and exact value of n are reported in the figure captions.

Supplementary Material

Refer to Web version on PubMed Central for supplementary material.

Acknowledgments

The authors would like to thank M. Karbowski (Univeristy of Maryland, Baltimore) for supplying the Drp1 vectors and N.G. Larsson (Max Planck Institute for Biology of Ageing, D-50931 Cologne, Germany) for supplying the mito-dsRed vector used in this study. We would also like to thank E. Bordt (University of Maryland School of Medicine) for discussion on the mitochondrial analysis. This work is supported by R01DA038613 to M.K.L and R01DA037257 to D.M.D. R.C. is supported by Brain and Behavior Research Foundation (NARSAD Young Investigator, P&S Fund). ME is supported by Mission Interministérielle de Lutte contre les Drogues Et les Conduites Addictives.

References

Bock R, Shin JH, Kaplan AR, Dobi A, Markey E, Kramer PF, Gremel CM, Christensen CH, Adrover MF, Alvarez VA. Strengthening the accumbal indirect pathway promotes resilience to compulsive cocaine use. Nat Neurosci. 2013; 16:632–638. [PubMed: 23542690]

Bordt EA, Clerc P, Roelofs BA, Saladino AJ, Tretter L, Adam-Vizi V, Cherok E, Khalil A, Yadava N, Ge SX, et al. The Putative Drp1 Inhibitor mdivi-1 Is a Reversible Mitochondrial Complex I Inhibitor that Modulates Reactive Oxygen Species. Dev Cell. 2017; 40:583–594. [PubMed: 28350990]

Cai N, Li Y, Chang S, Liang J, Lin C, Zhang X, Liang L, Hu J, Chan W, Kendler KS, et al. Genetic Control over mtDNA and Its Relationship to Major Depressive Disorder. Curr Biol. 2015; 25:3170–3177. [PubMed: 26687620]

Calipari ES, Bagot RC, Purushothaman I, Davidson TJ, Yorgason JT, Pena CJ, Walker DM, Pirpinias ST, Guise KG, Ramakrishnan C, et al. In vivo imaging identifies temporal signature of D1 and D2 medium spiny neurons in cocaine reward. Proc Natl Acad Sci USA. 2016; 113:2726–2731. [PubMed: 26831103]

Cassidy-Stone A, Chipuk JE, Ingerman E, Song C, Yoo C, Kuwana T, Kurth MJ, Shaw JT, Hinshaw JE, Green DR, Nunnari J. Chemical. Inhibition of the Mitochondrial Division Dynamin Reveals Its Role in Bax/Bak-Dependent Mitochondrial Outer Membrane Permeabilization. Dev Cell. 2008; 14:193–204. [PubMed: 18267088]

Cereghetti GM, Stangherlin A, Martins de Brito O, Chang CR, Blackstone C, Bernardi P, Scorrano L. Dephosphorylation by calcineurin regulates translocation of Drp1 to mitochondria. Proc Natl Acad Sci USA. 2008; 105:15803–15808. [PubMed: 18838687]

Chandra R, Francis TC, Konkalmatt P, Amgalan A, Gancarz AM, Dietz DM, Lobo MK. Opposing role for Egr3 in nucleus accumbens cell subtypes in cocaine action. J Neurosci. 2015; 35:7927–7937. [PubMed: 25995477]

Chandra R, Lenz JD, Gancarz AM, Chaudhury D, Schroeder GL, Han MH, Cheer JF, Dietz DM, Lobo MK. Optogenetic inhibition of D1R containing nucleus accumbens neurons alters cocaine-mediated regulation of Tiam1. Front Mol Neurosci. 2013; 6:13. [PubMed: 23745104]

Chandra R, Francis TC, Nam H, Riggs LM, Engeln M, Rudzinskas S, Konkalmatt P, Russo SJ, Turecki G, Iniguez SD, Lobo MK. Reduced Slc6a15 in Nucleus Accumbens D2-Neurons Underlies Stress Susceptibility. J Neurosci. 2017; 27:6527–6538.

Chang CR, Blackstone C. Cyclic AMP-dependent protein kinase phosphorylation of Drp1 regulates its GTPase activity and mitochondrial morphology. J Biol Chem. 2007; 282:21583–21587. [PubMed: 17553808]

Chen SD, Zhen YY, Lin JW, Lin TK, Huang CW, Liou CW, Chan SH, Chuang YC. Dynamin-Related Protein 1 Promotes Mitochondrial Fission and Contributes to The Hippocampal Neuronal Cell Death Following Experimental Status Epilepticus. CNS Neurosci Ther. 2016; 22:988–999. [PubMed: 27577016]

Cho B, Choi SY, Cho HM, Kim HJ, Sun W. Physiological and pathological significance of dynamin-related protein 1 (drp1)-dependent mitochondrial fission in the nervous system. Exp Neurobiol. 2013; 22:149–157. [PubMed: 24167410]

CONVERGE consortium. Sparse whole-genome sequencing identifies two loci for major depressive disorder. Nature. 2015; 523:588–591. [PubMed: 26176920]

Creed M, Ntamati NR, Chandra R, Lobo MK, Lüscher C. Convergence of Reinforcing and Anhedonic Cocaine Effects in the Ventral Pallidum. Neuron. 2016; 1:214–226.

Cunha-Oliveira T, Silva L, Silva AM, Moreno AJ, Oliveira CR, Santos MS. Mitochondrial complex I dysfunction induced by cocaine and cocaine plus morphine in brain and liver mitochondria. Toxicol Lett. 2013; 219:298–306. [PubMed: 23542814]

Damez-Werno DM, Sun H, Scobie KN, Shao N, Rabkin J, Dias C, Calipari ES, Maze I, Pena CJ, Walker DM, et al. Histone arginine methylation in cocaine action in the nucleus accumbens. Proc Natl Acad Sci. 2016; 113:9623–9628. [PubMed: 27506785]

Detmer SA, Chan DC. Functions and dysfunctions of mitochondrial dynamics. Nat Rev Mol Cell Biol. 2007; 8:870–879. [PubMed: 17928812]

Dietrich JB, Mangeol A, Revel MO, Burgun C, Aunis D, Zwiller J. Acute or repeated cocaine administration generates reactive oxygen species and induces antioxidant enzyme activity in dopaminergic rat brain structures. Neuropharmacology. 2005; 48:965–974. [PubMed: 15857623]

Dietz DM, Sun H, Lobo MK, Cahill ME, Chadwick B, Gao V, Koo JW, Mazei-Robison MS, Dias C, Maze I, Damez-Werno D, Dietz KC, Scobie KN, Ferguson D, Christoffel D, Ohnishi Y, Hodes GE, Zheng Y, Neve RL, Hahn KM, Russo SJ, Nestler EJ. Rac1 is essential in cocaine-induced structural plasticity of nucleus accumbens neurons. Nat Neurosci. 2012; 6:891–896.

Feng J, Wilkinson M, Liu X, Purushothaman I, Ferguson D, Vialou V, Maze I, Shao N, Kennedy P, Koo J, et al. Chronic cocaine-regulated epigenomic changes in mouse nucleus accumbens. Genome Biol. 2014; 15:R65. [PubMed: 24758366]

Ferguson SM, Eskenazi D, Ishikawa M, Wanat MJ, Phillips PE, Dong Y, Roth BL, Neumaier JF. Transient neuronal inhibition reveals opposing roles of indirect and direct pathways in sensitization. Nat Neurosci. 2011; 14:22–24. [PubMed: 21131952]

Francis TC, Chandra R, Gaynor A, Konkalmatt P, Metzbower SR, Evans B, Engeln M, Blanpied TA, Lobo MK. Molecular basis of dendritic atrophy and activity in stress susceptibility. Mol Psych. 2017; 22:1512–1519.

Friedman JR, Nunnari J. Mitochondrial form and function. Nature. 2014; 505:335–343. [PubMed: 24429632]

Gancarz AM, Wang ZJ, Schroeder GL, Damez-Werno D, Braunscheidel KM, Mueller LE, Humby MS, Caccamise A, Martin JA, Dietz KC, et al. Activin receptor signaling regulates cocaine-primed behavioral and morphological plasticity. Nat Neurosci. 2015; 18:959–961. [PubMed: 26030849]

Gerfen CR, Paletzki R, Heintz N. GENSAT BAC cre-recombinase driver lines to study the functional organization of cerebral cortical and basal ganglia circuits. Neuron. 2013; 80:1368–1383. [PubMed: 24360541]

Golden SA, Christoffel DJ, Heshmati M, Hodes GE, Magida J, Davis K, Cahill ME, Dias C, Ribeiro E, Ables JL, et al. Epigenetic regulation of RAC1 induces synaptic remodeling in stress disorders and depression. Nat Med. 2013; 19:337–344. [PubMed: 23416703]

Gong S, Doughty M, Harbaugh CR, Cummins A, Hatten ME, Heintz N, Gerfen CR. Targeting Cre recombinase to specific neuron populations with bacterial artificial chromosome constructs. J Neurosci. 2007; 27:9817–9823. [PubMed: 17855595]

Grueter BA, Robison AJ, Neve RL, Nestler EJ, Malenka RC. FosB differentially modulates nucleus accumbens direct and indirect pathway function. Proc Natl Acad Sci USA. 2013; 110:1923–1928. [PubMed: 23319622]

Graziane NM, Sun S, Wright WJ, Jang D, Liu Z, Huang YH, Nestler EJ, Wang YT, Schlüter OM, Dong Y. Opposing mechanisms mediate morphine- and cocaine-induced generation of silent synapses. Nat Neurosci. 19:915–925.

Hara Y, Yuk F, Puri R, Janssen WG, Rapp PR, Morrison JH. Presynaptic mitochondrial morphology in monkey prefrontal cortex correlates with working memory and is improved with estrogen treatment. Proc Natl Acad Sci USA. 2014; 111:486–491. [PubMed: 24297907]

Heiman M, Schaefer A, Gong S, Peterson JD, Day M, Ramsey KE, Suarez-Farinas M, Schwarz C, Stephan DA, Surmeier DJ, et al. A translational profiling approach for the molecular characterization of CNS cell types. Cell. 2008; 135:738–748. [PubMed: 19013281]

Hikida T, Kimura K, Wada N, Funabiki K, Nakanishi S. Distinct roles of synaptic transmission in direct and indirect striatal pathways to reward and aversive behavior. Neuron. 2010; 66:896–907. [PubMed: 20620875]

Hollis F, van der Kooij MA, Zanoletti O, Lozano L, Canto C, Sandi C. Mitochondrial function in the brain links anxiety with social subordination. Proc Natl Acad Sci USA. 2015; 112:15486–15491. [PubMed: 26621716]

Ingerman E, Perkins EM, Marino M, Mears JA, McCaffery JM, Hinshaw JE, Nunnari J. Dnm1 forms spirals that are structurally tailored to fit mitochondria. J Cell Biol. 2005; 7:1021–1027.

Ishihara N, Nomura M, Jofuku A, Kato H, Suzuki SO, Masuda K, Otera H, Nakanishi Y, Nonaka I, Goto Y, et al. Mitochondrial fission factor Drp1 is essential for embryonic development and synapse formation in mice. Nat Cell Biol. 2009; 11:958–966. [PubMed: 19578372]

Jang EY, Ryu YH, Lee BH, Chang SC, Yeo MJ, Kim SH, Folsom RJ, Schilaty ND, Kim KJ, Yang CH, et al. Involvement of reactive oxygen species in cocaine-taking behaviors in rats. Addict Biol. 2015; 20:663–675. [PubMed: 24975938]

Kalivas PW. The glutamate homeostasis hypothesis of addiction. Nat Rev Neurosci. 2009; 10:561–572. [PubMed: 19571793]

Kim J, Park BH, Lee JH, Park SK, Kim JH. Cell type-specific alterations in the nucleus accumbens by repeated exposures to cocaine. Biol Psychiatry. 2011; 69:1026–1034. [PubMed: 21377654]

Kim H, Lee JY, Park KJ, Kim WH, Roh GS. A mitochondrial division inhibitor, Mdivi-1, inhibits mitochondrial fragmentation and attenuates kainic acid-induced hippocampal cell death. BMC Neurosci. 2016; 17:33. [PubMed: 27287829]

Labrousse AM, Zappaterra MD, Rube DA, van der Bliek AM. C. elegans dynamin-related protein DRP-1 controls severing of the mitochondrial outer membrane. Mol Cell. 1999; 5:815–826.

Lee BR, Ma YY, Huang YH, Wang X, Otaka M, Ishikawa M, Neumann PA, Graziane NM, Brown TE, Suska A, et al. Maturation of silent synapses in amygdala-accumbens projection contributes to incubation of cocaine craving. Nat Neurosci. 2013; 16:1644–1651. [PubMed: 24077564]

Lehrmann E, Oyler J, Vawter MP, Hyde TM, Kolachana B, Kleinman JE, Huestis MA, Becker KG, Freed WJ. Transcriptional profiling in the human prefrontal cortex: evidence for two activational states associated with cocaine abuse. Pharmacogenomics J. 2003; 3:27–40. [PubMed: 12629581]

Li H, Chen Y, Jones AF, Sanger RH, Collis LP, Flannery R, McNay EC, Yu T, Schwarzenbacher R, Bossy B, Bossy-Wetzel E, Bennett MV, Pypaert M, Hickman JA, Smith PJ, Hardwick JM, Jonas EA. Bcl-xL induces Drp1-dependent synapse formation in cultured hippocampal neurons. Proc Natl Acad Sci USA. 2008; 6:2169–2174.

Li X, Rubio FJ, Zeric T, Bossert JM, Kambhampati S, Cates HM, Kennedy PJ, Liu QR, Cimbro R, Hope BT, et al. Incubation of methamphetamine craving is associated with selective increases in expression of Bdnf and trkb, glutamate receptors, and epigenetic enzymes in cue-activated fos-expressing dorsal striatal neurons. J Neurosci. 2015; 35:8232–8244. [PubMed: 26019338]

Li Z, Okamoto K, Hayashi Y, Sheng M. The importance of dendritic mitochondria in the morphogenesis and plasticity of spines and synapses. Cell. 2004; 119:873–887. [PubMed: 15607982]

Lobo MK, Covington HE 3rd, Chaudhury D, Friedman AK, Sun H, Damez-Werno D, Dietz DM, Zaman S, Koo JW, Kennedy PJ, et al. Cell type-specific loss of BDNF signaling mimics optogenetic control of cocaine reward. Science. 2010; 330:385–390. [PubMed: 20947769]

Lobo MK, Nestler EJ. The striatal balancing act in drug addiction: distinct roles of direct and indirect pathway medium spiny neurons. Front Neuroanat. 2011; 5:41. [PubMed: 21811439]

Lobo MK, Zaman S, Damez-Werno DM, Koo JW, Bagot RC, DiNieri JA, Nugent A, Finkel E, Chaudhury D, Chandra R, et al. DeltaFosB induction in striatal medium spiny neuron subtypes in response to chronic pharmacological, emotional, and optogenetic stimuli. J Neurosci. 2013; 33:18381–18395. [PubMed: 24259563]

MacAskill AF, Cassel JM, Carter AG. Cocaine exposure reorganizes cell type- and input-specific connectivity in the nucleus accumbens. Nat Neurosci. 2014; 17:1198–1207. [PubMed: 25108911]

Manji H, Kato T, Di Prospero NA, Ness S, Beal MF, Krams M, Chen G. Impaired mitochondrial function in psychiatric disorders. Nat Rev Neurosci. 2012; 13:293–307. [PubMed: 22510887]

Maze I, Wenderski W, Noh KM, Bagot RC, Tzavaras N, Purushothaman I, Elsässer SJ, Guo Y, Ionete C, Hurd YL, et al. Critical Role of Histone Turnover in Neuronal Transcription and Plasticity. Neuron. 2015; 87:77–94. [PubMed: 26139371]

Pascoli V, Terrier J, Espallergues J, Valjent E, O'Connor EC, Luscher C. Contrasting forms of cocaine-evoked plasticity control components of relapse. Nature. 2014; 509:459–464. [PubMed: 24848058]

Patton MH, Roberts BM, Lovinger DM, Mathur BN. Ethanol Disinhibits Dorsolateral Striatal Medium Spiny Neurons Through Activation of A Presynaptic Delta Opioid Receptor. Neuropsychopharm. 7:1831–1840.

Paxinos, G., Franklin, KBJ. The Mouse Brain in Stereotaxic Coordinates. Second Edition. Academic Press; 2001.

Picard M, McManus MJ, Gray JD, Nasca C, Moffat C, Kopinski PK, Seifert EL, McEwen BS, Wallace DC. Mitochondrial functions modulate neuroendocrine, metabolic, inflammatory, and transcriptional responses to acute psychological stress. Proc Natl Acad Sci USA. 2015; 112:E6614–6623. [PubMed: 26627253]

Pomierny-Chamiolo L, Moniczewski A, Wydra K, Suder A, Filip M. Oxidative stress biomarkers in some rat brain structures and peripheral organs underwent cocaine. Neurotox Res. 2013; 23:92–102. [PubMed: 22791409]

Prasad KM, Smith RS, Xu Y, French BA. A single direct injection into the left ventricular wall of an adeno-associated virus 9 (AAV9) vector expressing extracellular superoxide dismutase from the cardiac troponin-T promoter protects mice against myocardial infarction. J Gene Med. 2011; 6:333–341.

Robison AJ, Vialou V, Mazei-Robison M, Feng J, Kourrich S, Collins M, Wee S, Koob G, Turecki G, Neve R, et al. Behavioral and structural responses to chronic cocaine require a feedforward loop involving DeltaFosB and calcium/calmodulin-dependent protein kinase II in the nucleus accumbens shell. J Neurosci. 2013; 33:4295–4307. [PubMed: 23467346]

Sanz E, Yang L, Su T, Morris DR, McKnight GS, Amieux PS. Cell-type-specific isolation of ribosome-associated mRNA from complex tissues. Proc Natl Acad Sci USA. 2009; 106:13939–13944. [PubMed: 19666516]

Shuen JA, Chen M, Gloss B, Calacos N. Drd1a-tdTomato BAC transgenic mice for simultaneous visualization of medium spiny neurons in the direct and indirect pathways of the basal ganglia. J Neurosci. 2008; 11:2681–2685.

Smith RJ, Lobo MK, Spencer S, Kalivas PW. Cocaine-induced adaptations in D1 and D2 accumbens projection neurons (a dichotomy not necessarily synonymous with direct and indirect pathways). Curr Opin Neurobiol. 2013; 23:546–552. [PubMed: 23428656]

Steib K, Schaffner I, Jagasia R, Ebert B, Lie DC. Mitochondria modify exercise-induced development of stem cell-derived neurons in the adult brain. J Neurosci. 2014; 34:6624–6633. [PubMed: 24806687]

Sterky FH, Lee S, Wibom R, Olson L, Larsson NG. Impaired mitochondrial transport and Parkin-independent degeneration of respiratory chain-deficient dopamine neurons in vivo. Proc Natl Acad Sci USA. 2011; 108:12937–12942. [PubMed: 21768369]

Sun H, Damez-Werno DM, Scobie KN, Shao NY, Dias C, Rabkin J, Koo JW, Korb E, Bagot RC, Ahn FH, et al. ACF chromatin-remodeling complex mediates stress-induced depressive-like behavior. Nat Med. 2015; 21:1146–1153. [PubMed: 26390241]

Sun H, Martin JA, Werner CT, Wang ZJ, Damez-Werno DM, Scobie KN, Shao NY, Dias C, Rabkin J, Koo JW, et al. BAZ1B in Nucleus Accumbens Regulates Reward-Related Behaviors in Response to Distinct Emotional Stimuli. J Neurosci. 2016; 36:3954–3961. [PubMed: 27053203]

Taguchi N, Ishihara N, Jofuku A, Oka T, Mihara K. Mitotic phosphorylation of dynamin-related GTPase Drp1 participates in mitochondrial fission. J Biol Chem. 2007; 282:11521–11529. [PubMed: 17301055]

Tanaka A, Youle RJ. A chemical inhibitor of DRP1 uncouples mitochondrial fission and apoptosis. Mol Cell. 2008; 29:409–410. [PubMed: 18313377]

van der Kooij MA, Hollis F, Lozano L, Zalachoras I, Abad S, Zanoletti O, Grosse J, Guillot de Suduiraut I, Canto C, Sandi C. Mol Psych. 2017; doi: 10.1038/mp.2017.135

Volkow ND, Fowler JS, Wolf AP, Hitzemann R, Dewey S, Bendriem B, Alpert R, Hoff A. Changes in brain glucose metabolism in cocaine dependence and withdrawal. Am J Psychiatry. 1991; 148:621–626. [PubMed: 2018164]

Werner CT, Milovanovic M, Christian DT, Loweth JA, Wolf ME. Response of the Ubiquitin-Proteasome System to Memory Retrieval After Extended-Access Cocaine or Saline Self-Administration. Neuropsychopharmacology. 2015; 40:3006–3014. [PubMed: 26044907]

Westermann B. Mitochondrial fusion and fission in cell life and death. Nat Rev Mol Cell Biol. 2010; 11:872–884. [PubMed: 21102612]

Wilson CJ, Groves PM, Kitai ST, Linder JC. Three-dimensional structure of dendritic spines in the rat neostriatum. J Neurosci. 1983; 3:383–388. [PubMed: 6822869]

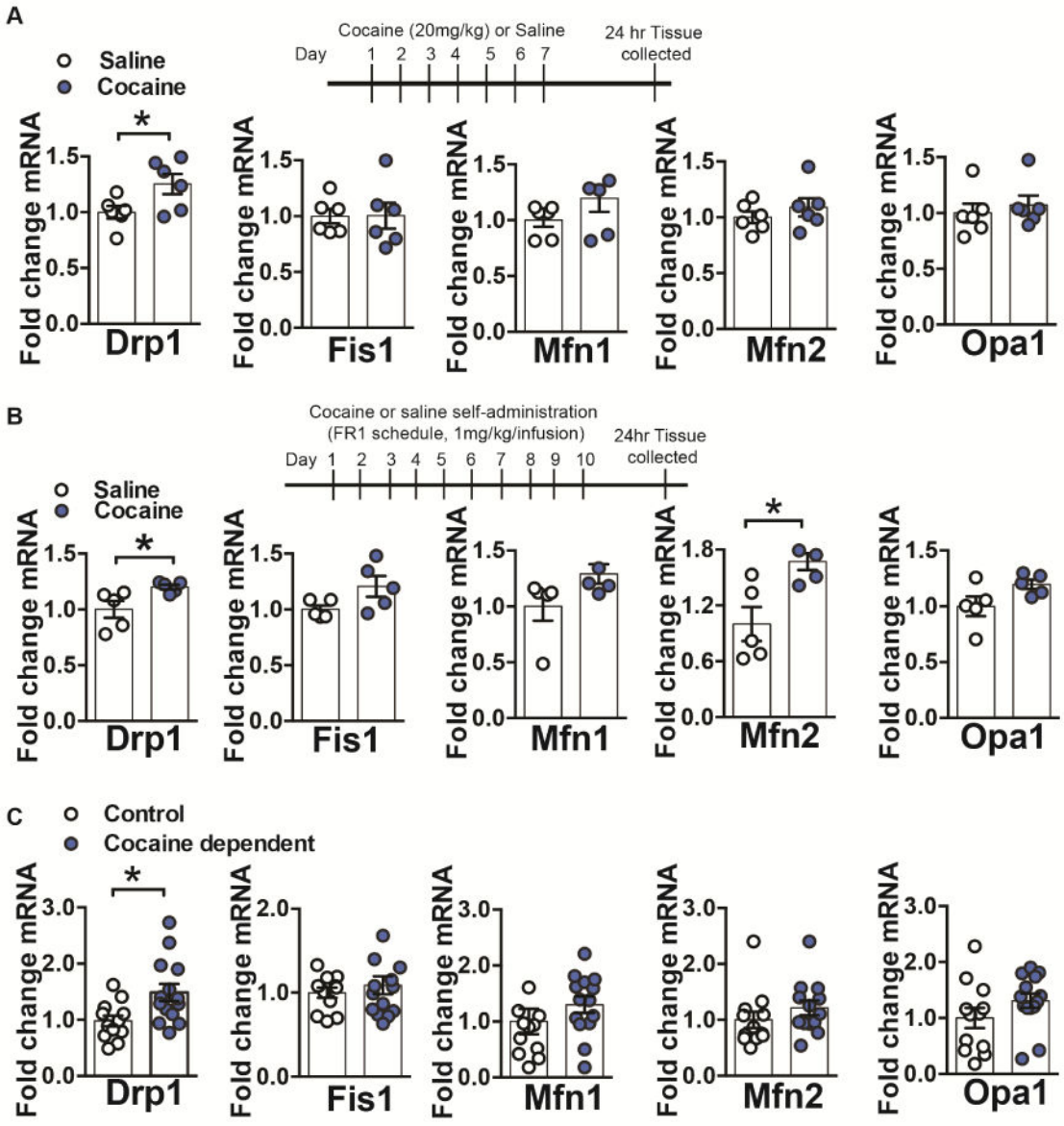

Figure 1. Dynamin-related protein 1 (Drp1) mRNA expression is increased in NAc after repeated cocaine and postmortem NAc of cocaine dependents

(A) Repeated cocaine (7 days, 20mg/kg, ip) caused an increase in Drp1 mRNA in NAc, compared to saline treated controls Student's t test: t=2.378, df=10, p=0.03. However, mRNA of other mitochondrial fission (Fis1) or fusion (Mfn1, Mfn2, and Opa1) genes were unaltered in NAc in cocaine vs. saline groups: Student's t-test (in the order of the genes displayed): t=0.03, df=10, p=0.97, t=1.46, df=10, p=0.17, t=0.91, df=10, p=0.38, t=0.58, df=10, p=0.56. n=6 in each group. **(B)** Drp1 mRNA is increased in NAc of rats after cocaine self-administration (1mg/kg/infusion, 10 days, FR1 schedule) Student's t test, t=2.542, df=8, p=0.03. While mRNA for other mitochondrial fission or fusion genes was unaltered after cocaine self-administration: Student's t-test (in the order of the genes displayed): t=2.08, df=8, p=0.07, t=1.86, df=8, p=0.09, t=2.01, df=8, p=0.08, only Mfn2 showed significantly increased levels: Student's t-test: t=3.14, df=7, p=0.01. n=5 in each group. **(C)** Drp1 mRNA

was increased in postmortem NAc of cocaine dependents (Student's t test, t=2.707, df=24, p=0.01) but mRNA for other mitochondrial fission or fusion genes was unchanged: Student's t-test (in the order of the genes displayed): t=0.69, df=24, p=0.49, t=1.15, df=24, p=0.26, t=1.09, df=24, p=0.28, t=1.42, df=24, p=0.16. n=12 control and 14 cocaine dependent. *p<0.05. Error bars, SEM. See also Table S1 and Figure S1.

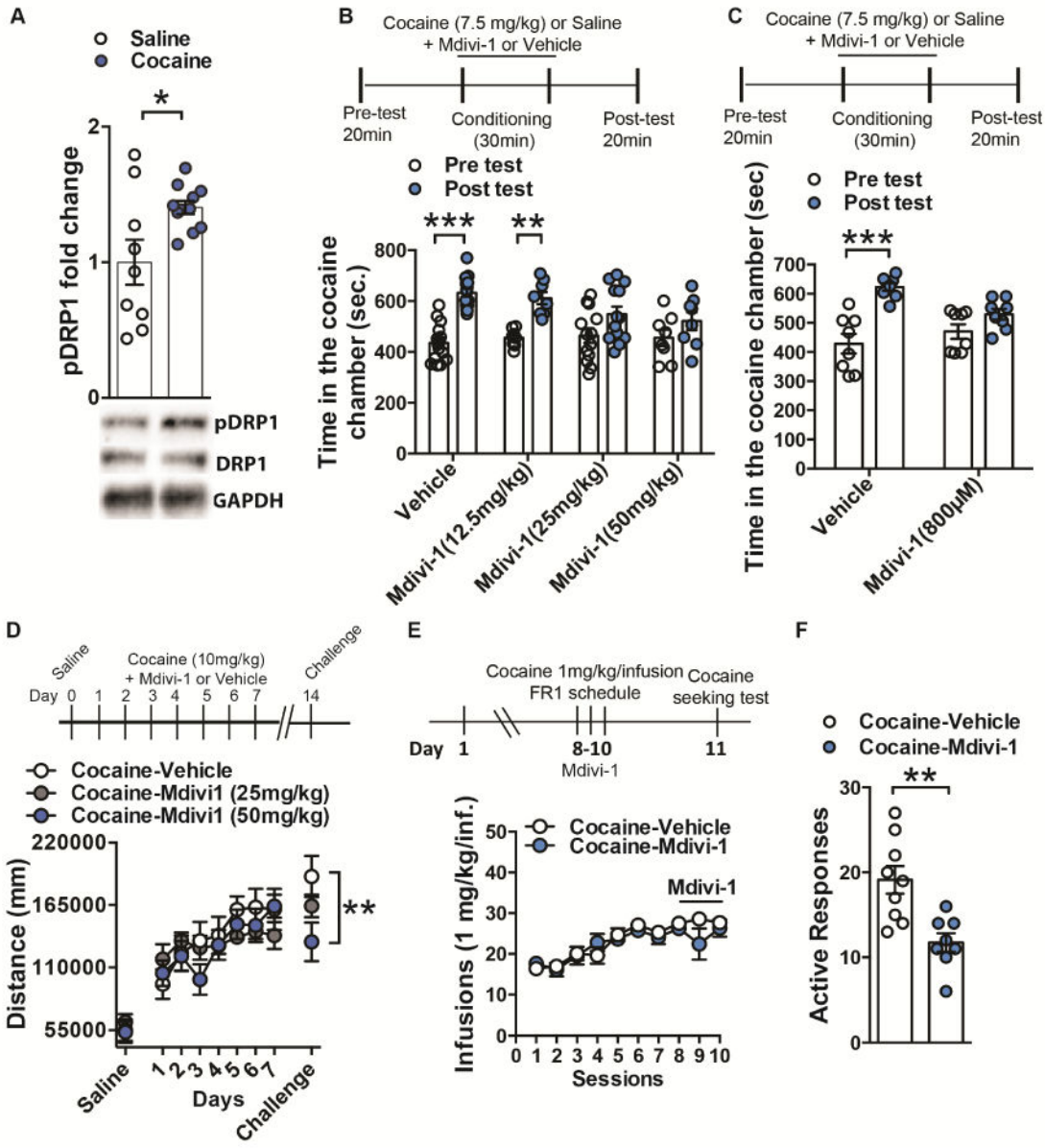

Figure 2. Inhibiting mitochondrial fission with Mdivi-1 reduces cocaine behavioral outcomes

(A) pSer616-Drp1 is increased in NAc after repeated cocaine (7 days, 20mg/kg, ip) compared to saline controls. pSer616-Drp1 levels were normalized to total Drp1 and GAPDH. Student's t-test, t=2.551, df=18, p=0.02, n=9 saline and 11 cocaine **(B)** Mice pre-treated with both 25mg/kg (n=13) and 50mg/kg (n=8) did not display a change in time spent in the drug paired chamber post cocaine conditioning, whereas vehicle (n=15) and 12.5mg/kg (n=8) displayed a significant increased in time spent in the drug paired chamber post conditioning: Two-way Repeated Measure ANOVA: Time: $F_{(1,40)}$=43.87, p<0.0001, Tukey post-hoc: p<0.001 and p<0.01 respectively. **(C)** Mice pretreated with Mdivi-1 infusion in the NAc (800μM/0.5μL/side) failed to show cocaine conditioned place preference when comparing time in the drug-paired chamber before and after conditioning, contrary to vehicle-treated animals: Two-way Repeated Measure ANOVA: Time: $F_{(1,14)}$=44.81,

p<0.0001, Tukey post-hoc: p<0.001; n=8 in each group. **(D)** Cocaine (10mg/kg)-induced locomotion was unaltered with 25mg/kg (n=7) or 50mg/kg (n=7) Mdivi-1 treatment compared to vehicle control (n=10). However, mice pretreated with 50mg/kg Mdivi-1 show reduced locomotor sensitization, compared to saline controls, when challenged with cocaine (10mg/kg) 7 days after withdrawal (Two-way Repeated Measures ANOVA: Interaction: $F_{(16,176)}$=1.79, p=0.0356, Tukey post-hoc: p<0.01). **(E)** Rats receiving NAc infusion of Mdivi-1 (800μM; 1 μL/side; n=8) during the last 3 FR1 sessions of cocaine self-administration show similar cocaine intake compared to control group (n=9): Two-way Repeated Measures ANOVA: Interaction: $F_{(9,150)}$=1.089, p=0.37. **(F)** When tested for cocaine seeking, 24h after the last FR1session and Mdivi-1 infusion, treated rats showed reduced responding: Student's t-test, t=3.66, df=15; p=0.002. *p<0.05. Error bars, SEM. See also Figure S2.

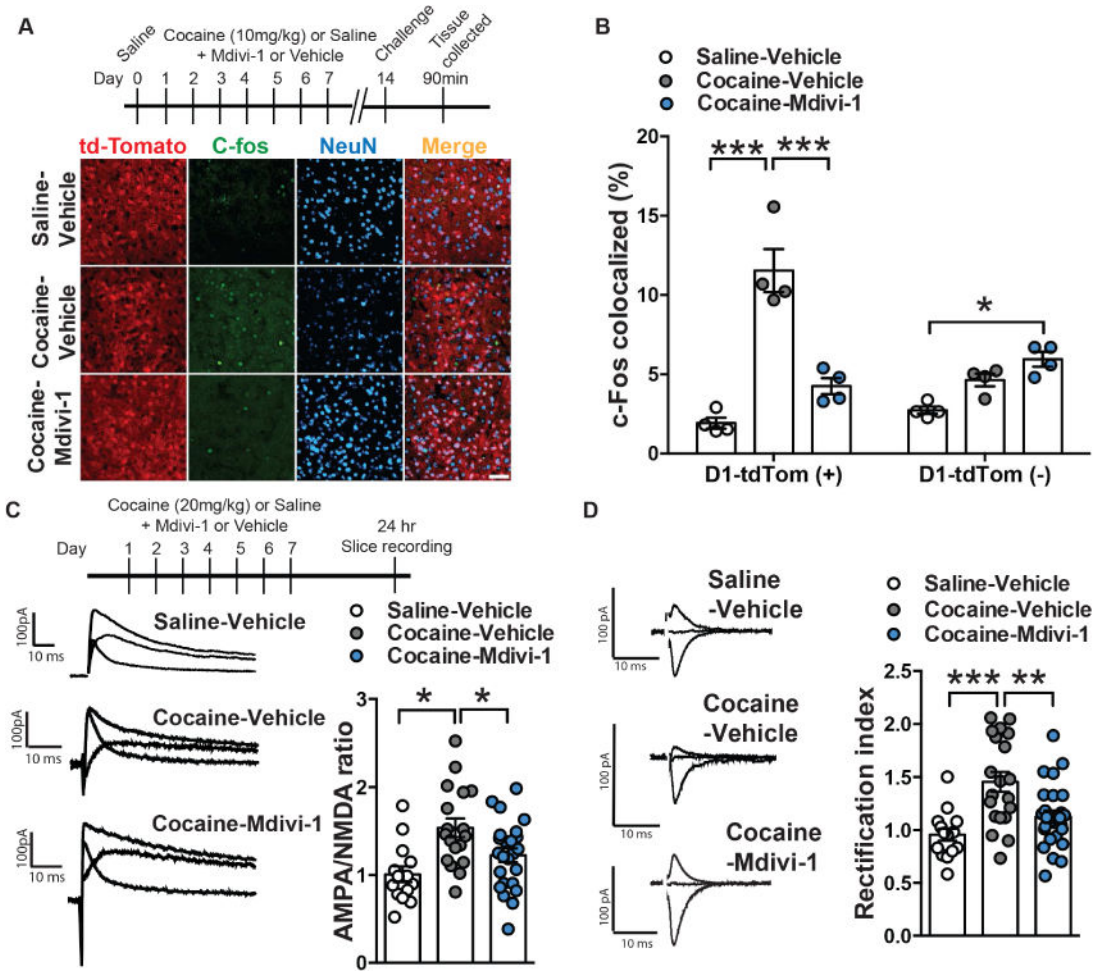

Figure 3. Inhibiting mitochondrial fission with Mdivi-1 reduces cocaine-induced D1-MSN adaptations

(A) Representative confocal images of D1-MSNs (red), c-Fos (green) and neuronal marker NeuN (blue) in Saline-Vehicle (top), Cocaine-Vehicle (middle) and Cocaine-Mdivi-1 (bottom) groups. Scale bar: 50μm. **(B)** Mdivi-1 (50mg/kg, ip) reduced cocaine-induced c-Fos colocalization in D1-MSNs and leads to a modest increase of c-Fos colocalization in non-D1-MSN cells when compared to saline-vehicle controls. Two-way ANOVA: Interaction: $F_{(2,18)}$=25.41, p<0.0001, Tukey post-hoc: p<0.001 and p<0.05 respectively. n=4 in each group. **(C)** Representative traces of AMPA/NMDA ratio in D1-MSNs of mice pre-treated with vehicle and receiving saline, mice pre-treated with vehicle receiving cocaine and mice pre-treated with Mdivi-1 receiving cocaine (left panel). Mdivi-1 (50mk/kg, ip) normalized cocaine-induced increase in AMPA/NMDA ratio: One-way ANOVA: $F_{(2,53)}$=7.214, p=0.0017, Tukey post-hoc: p<0.05. Saline-Vehicle: n=14 cells, Cocaine-Vehicle: n=18 cells and Cocaine-Mdivi-1: n=24 cells, all obtained from 6 mice in each group (right panel). **(D)** Representative traces of rectification index in saline-vehicle (top), cocaine-vehicle (middle) and cocaine-Mdivi-1 (bottom) pre-treated mice (left panel). Quantification of AMPA current rectification index (RI): cocaine increased the RI relative to saline-treated controls, while Mdivi-1 treatment (50mg/kg, ip) reduced the RI in cocaine treated mice: One-way ANOVA: $F_{(2,58)}$=11.01, p<0.0001, Tukey post-hoc: p<0.001 and p<0.01; Saline-

Vehicle: n=15 cells, Cocaine-Vehicle: n=20 cells and Cocaine-Mdivi-1: n=26 cells, all obtained from 6 mice in each group (right panel). *p<0.05, **p<0.01, ***p<0.001. Error bars, SEM. See also Figure S3.

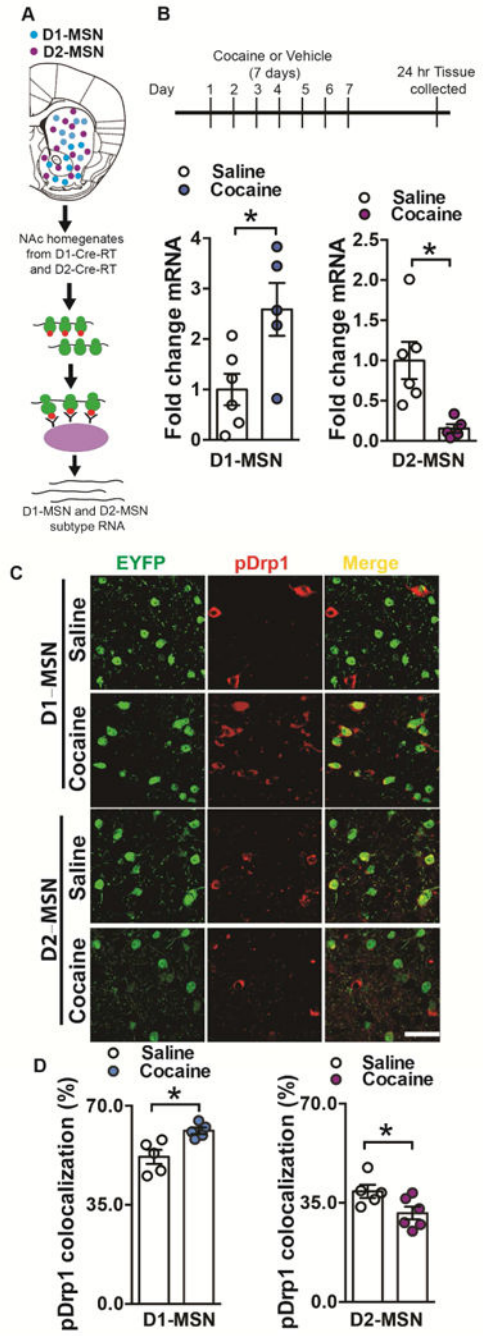

Figure 4. Drp1 ribosome associated mRNA is bidirectionally altered in MSN subtypes after repeated cocaine

(A) Illustration of NAc D1-MSN (blue) and D2-MSN (magenta) subtypes and the RiboTag procedure to isolate ribosome-associated mRNA from MSN subtypes using D1-Cre-RT and D2-Cre-RT mice. HA tagged (red) ribosomes are immunoprecipitated from NAc homogenates using anti-HA coupled to magnetic beads, followed by isolation of ribosome-associated mRNA from D1-MSNs and D2-MSNs. **(B)** Drp1 ribosome-associated mRNA is increased in D1-MSNs but reduced in D2-MSNs of D1-Cre-RT or D2-Cre-RT NAc after repeated cocaine (7 days, 20mg/kg). Student's t test, t=2.711, df=9, p=0.02 and t=3.251,

df=9, p=0.009 respectively. n=5 saline, 6 cocaine in both D1- and D2-MSNs groups. **(C)** Representative confocal images of pDrp1 immunostaining (red) in EYFP labeled D1- and D2-MSNs (green) following cocaine (or saline) 7 days treatment (20mg/kg, ip). Scale bar: 50μm. **(D)** Drp1 phosphorylation at Ser616 colocalization is increased in D1-MSNs (Student's t-test: t=3.338, df=8, p=0.01; n=5 in each group) and decreased in D2-MSNs (Student's t-test: t=2.355, df=9, p=0.04; n=5 saline and 6 cocaine) following cocaine repeated treatment. *p<0.05. Error bars, SEM. See also Figure S4.

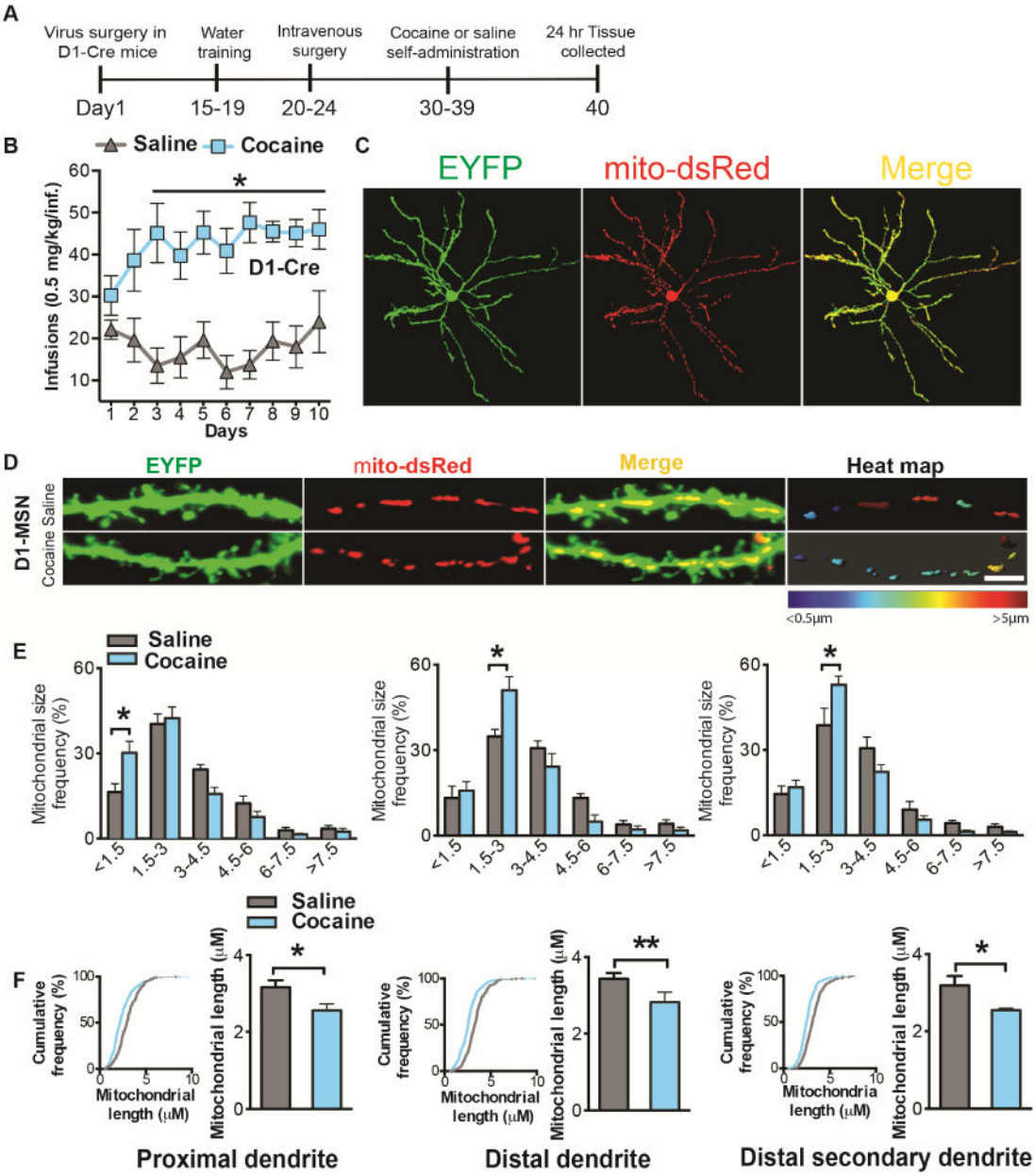

Figure 5. NAc D1-MSNs show decreased mitochondria size following cocaine self-administration

(A) Timeline of virus injection into NAc and cocaine self-administration in D1-Cre mice. Animals first receive Cre inducible virus to label MSN cell bodies (EYFP) and mitochondria (mito-dsRed). Two weeks later they were trained for water self-administration (FR1) for 4 days, followed by catheterization surgery. After recovery, mice self-administered cocaine (FR1) for 10 consecutive days. Finally, tissue was collected 24h following the last session. **(B)** D1-Cre mice developed stable cocaine intake (0.5mg/kg/infusion) from day 3 onward compared to saline controls (n=8 in each group): Two-way Repeated Measures ANOVA: Interaction: $F_{(9,126)}=2.913$, p=0.0036, Tukey post-hoc: $p<0.05$. **(C)** Representative confocal images of a D1-MSN co-labeled with EYFP (green) and mito-dsRed (red). **(D)** Representative confocal images of D1-MSN dendrites (green) with labeled mitochondria

(red) after cocaine or saline self-administration (left and middle panels). The right panel displays a heat map of mitochondrial length in MSN dendrites in cocaine and saline conditions. Scale bar 5μm. **(E)** 3D reconstruction of dendrites and mitochondria demonstrates an increase in the frequency of smaller length mitochondria in D1-MSN proximal (left; Two-way ANOVA: Interaction: $F_{(5,48)}$=4.04, p=0.0039, Bonferroni post-hoc: p<0.01.), distal (middle; Two-way ANOVA: Interaction: $F_{(5,48)}$=3.839, p=0.0053, Bonferroni post-hoc: p<0.01), and distal (right; Two-way ANOVA: Interaction: $F_{(5,48)}$=4.51, p=0.0019, Bonferroni post-hoc: p<0.01) secondary dendrites in the cocaine group (n=6) compared to saline controls (n=4). **(F)** Cumulative frequency distribution plots. A shift to the left is observed in D1-MSN dendrites implicating overall reduced mitochondrial length in D1-MSNs. Kolmogorov-Smirnov test: the maximum difference between the cumulative distributions D=0.19, 0.21 and 0.19μm in D1-MSN proximal, distal and distal secondary dendrites respectively, p<0.0001. The overall length of mitochondria is reduced in D1-MSN proximal (Student's t-test: t=2.337, df=8, p=0.04), distal (Student's t-test: t=4.969, df=8, p=0.001) and distal secondary (Student's t-test: t=2.911, df=8, p=0.02) dendrites in the cocaine (n=6) group as compared to saline (n=4). *p<0.05, **p<0.01. Error bars, SEM. See also Figure S5.

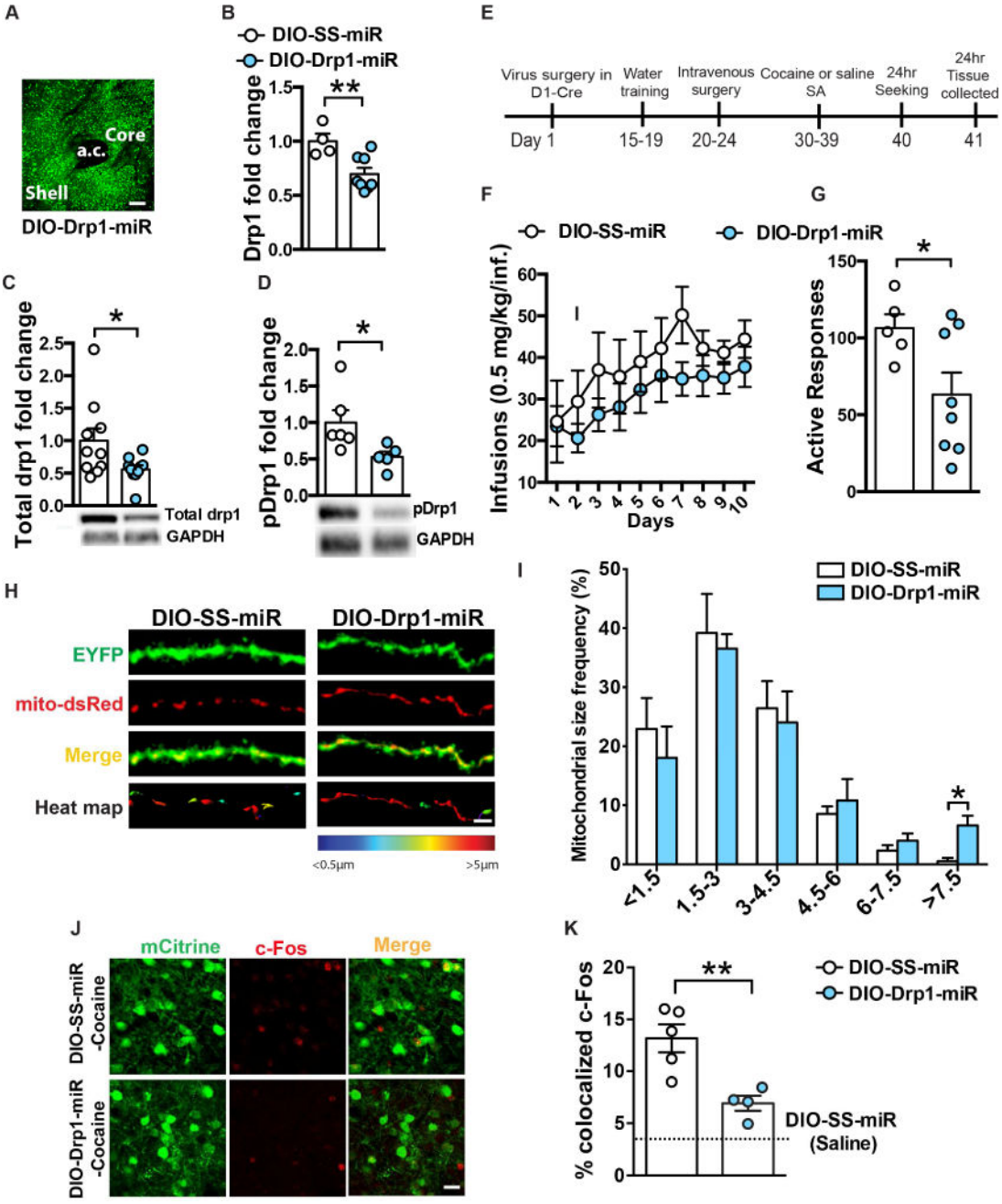

Figure 6. Blocking mitochondrial fission through Drp1 knockdown decreases cocaine seeking

(A) Representative confocal image of AAV-DIO-Drp1-miR expression in the NAc of D1-Cre mice. Scale bar: 100µm. **(B)** Virally-mediated Drp1 knockdown reduced Drp1 mRNA (31%, Student's t-test: t=3.241, df= 10, p=0.008; n=4 SS-miR and 8 Drp1-miR), **(C)** Total Drp1 (Student's t-test: t=2.214, df=18, p=0.04; n=10 in each group) and **(D)** pDrp1 are reduced (44% and 47% respectively in NAc after Drp1-miR expression in D1-MSNs (Student's t-test: t=2.373, df=9, p=0.04; n=6 SS-miR and 5 Drp1-miR) levels. **(E)** Timeline of the experiment: cocaine seeking was performed 24h after the last FR1 session. **(F)** Drp1 knockdown in NAc D1-MSNs had no effect on cocaine self-administration (FR1, 0.5mg/kg/

inf): Two-way Repeated Measures ANOVA: Interaction: $F_{(9,99)}$=0.4373, p=0.9118, but **(G)** decreased cocaine seeking 24h after the last FR1 session: Student's t-test: t=2.208, df=11, p=0.04; n=5 scramble and 8 Drp1-miR. **(H)** Representative confocal images of D1-MSN dendrites (green) with labeled mitochondria (red) after cocaine self-administration from SS-miR and Drp1-miR groups. Scale bar: 5μm. **(I)** Blocking mitochondrial fission increased the frequency of longer size mitochondria (>7.5 μm) in the dendrites of D1-MSNs (Student's t-test: t=3.142, df=7, p=0.01; n=4 scramble and 5 Drp1-miR). **(J)** Representative confocal images of D1-MSNs labeled with mCitrine (green) showing c-Fos (red) colocalization. Scale bar: 25μm. **(K)** Drp1 knockdown reduces cocaine-induced c-Fos expression in D1-MSNs: One-way ANOVA: $F_{(2,9)}$=19.9, p=0.0005. Scramble-Saline n=3, Scramble-Cocaine n=5, Drp1-miR n= 4. *p<0.05, **p<0.01. Error bars, SEM. See also Figure S6.

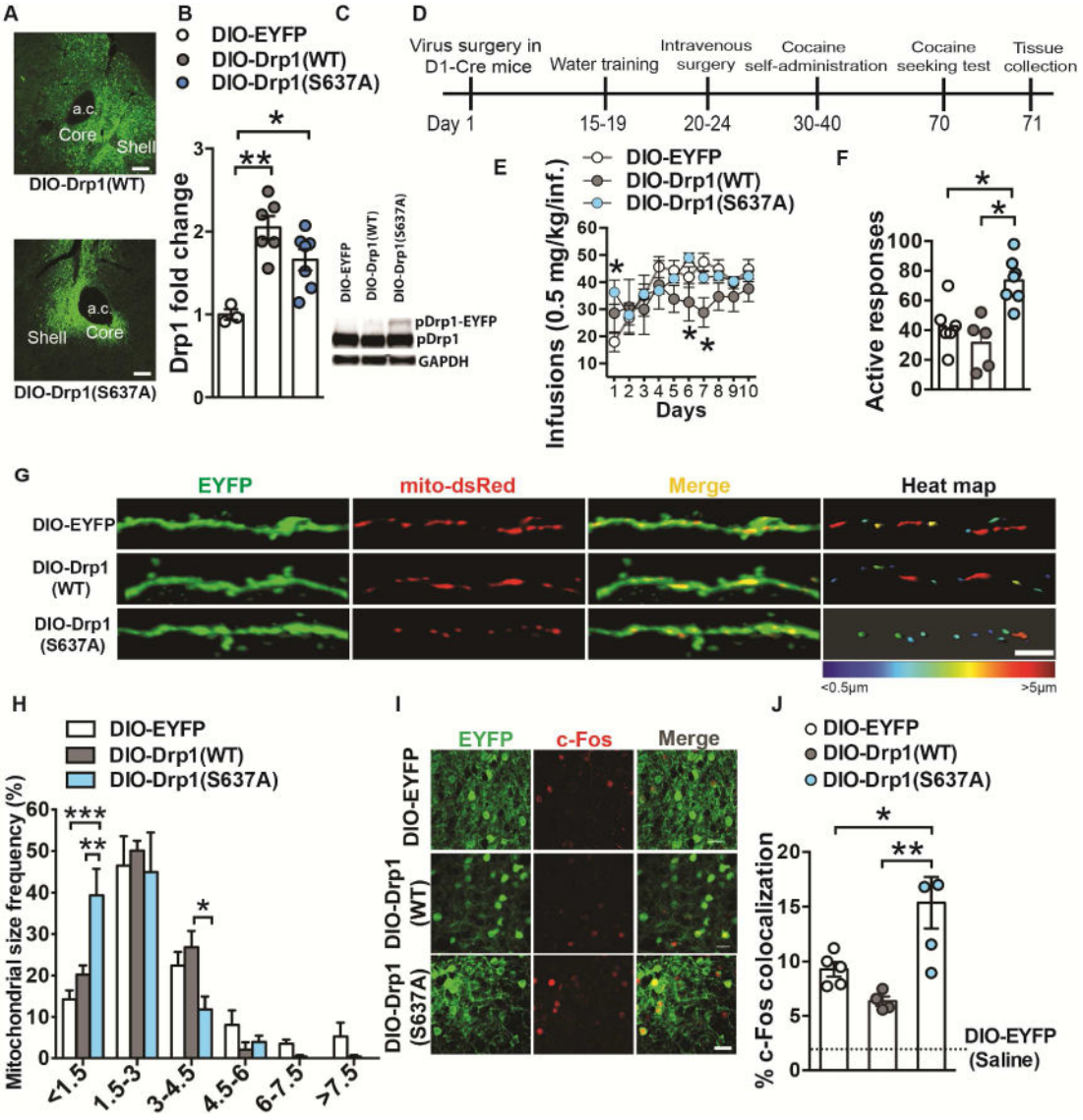

Figure 7. Enhancing fission promoting Drp1 in D1-MSNs increases acquisition to cocaine self-administration and seeking after long-term abstinence

(A) Conditional expression of DIO-Drp1(WT)-EYFP and DIO-Drp1(S637A)-EYFP in the nucleus accumbens. Scale bar, 100µm. **(B)** AAV delivery of DIO-Drp1(WT)-EYFP and DIO-Drp1(S637A)-EYFP to NAc of D2-Cre mice results in an increase of Drp1 mRNA. One-way ANOVA: $F_{(2,13)}$=11.15, p=0.0015, Tukey post-hoc: p<0.01 and p<0.05, n=3, 6 and 7 respectively. **(C)** NAc of D2-Cre mice receiving DIO-Drp1(S637A)-EYFP display an additional p-Ser616-Drp1-EYFP fusion protein band while DIO-EYFP and DIO-Drp1(WT)-EYFP mice do not display this band. GAPDH was used as a loading control. **(D)** Timeline of virus surgery, water training, cocaine self-administration, and seeking test. **(E)** Overexpression of Drp1(S637A)-EYFP in D1-MSNs resulted in higher cocaine intake on day 1 of self-administration compared to EYFP controls. Drp1(WT) expression attenuated cocaine intake on days 6 and 7 compared to Drp1(S637A)-EYFP and EYFP groups respectively: Two-way Repeated Measures ANOVA: Interaction $F_{(18,144)}$=1.896: p=0.02,

Tukey post-hoc: $p<0.05$. n=7, 5 and 7 respectively. **(F)** Overexpression of Drp1-S637A in D1-MSNs resulted in increased drug seeking 30 days after the last cocaine self-administration session: One-way ANOVA $F_{(2,16)}=11.22$, $p<0.01$ Tukey post-hoc: $p<0.05$. **(G)** Representative confocal images of D1-MSN dendrites (green) with labeled mitochondria (red) after cocaine self-administration of mice inject with AAV-DIO-EYFP (top), AAV-DIO-Drp1(WT)-EYFP (middle) and AAV-DIO-Drp1(S637A)-EYFP (bottom) vectors. The right panel displays a heat map of mitochondrial length in MSN dendrites in cocaine and saline conditions. Scale bar 5μm. **(H)** Mice expressing the constitutively active form of Drp1 (AAV-DIO-Drp1(S637A)-EYFP) showed increased smaller size mitochondria (<1.5μm) as well as increased longer size mitochondria (3–4.5μm): Two-way ANOVA: Interaction $F_{(10,72)}=3.530$: $p<0.0008$, Tukey post-hoc: $p<0.05$, $p<0.01$, $p<0.001$. n=5 in each group. **(I)** Representative confocal images of D1-MSNs labeled with EYFP (green) and c-Fos (red) from mice expressing EYFP (top), Drp1(WT)-EYFP (middle) or Drp1(S637A)-EYFP (bottom). Scale bar 25μm. **(J)** Overexpression of the constitutively active form of Drp1 (AAV-DIO-Drp1(S637A)-EYFP) increased drug-induced c-Fos colocalization in D1-MSNs of mice that received cocaine (20mg/kg, ip, 10 days) compared to AAV-DIO-EYFP and AAV-DIO-Drp1(WT)-EYFP. All cocaine groups displayed a significant increase in D1-MSN and c-Fos colocalization compared to saline AAV-DIO-EYFP controls: One-way ANOVA $F_{(2,11)}=8.771$, $p=0.005$, Tukey post-hoc: $p<0.05$, $p<0.01$. AAV-DIO-EYFP (n=5), AAV-DIO-Drp1(WT)-EYFP (n=4) and AAV-DIO-Drp1(S637A)-EYFP (n=5). *$p<0.05$, **$p<0.01$, ***$p<0.001$. Error bars, SEM. See also Figure S7.

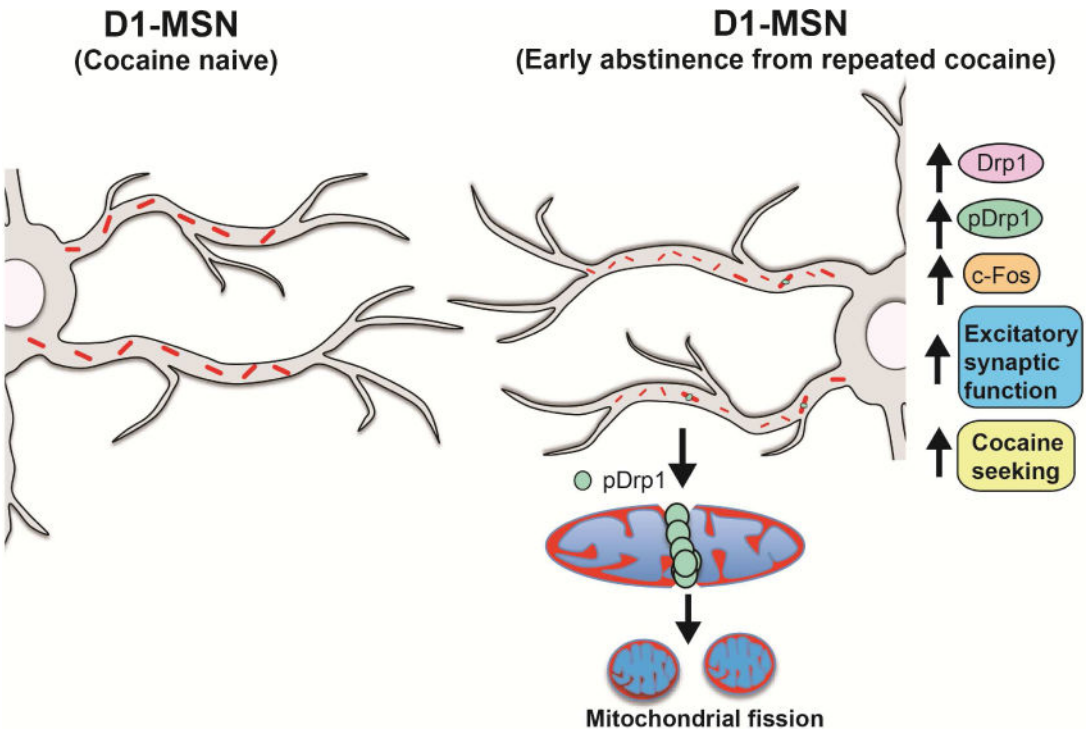

Figure 8. Model of Drp1-mediated mitochondrial fission in D1-MSNs during early abstinence from repeated cocaine

In NAc D1-MSNs, repeated cocaine exposure increases Drp1 levels. Enhanced phosphorylation of Drp1 at Ser616 leads to an abundance of smaller mitochondria, reflective of enhanced fission, in D1-MSN dendrites. The enhanced mitochondrial fission in D1-MSN dendrites is associated with increased c-Fos reactivity and increased excitatory synaptic function in this MSN subtype. These adaptations ultimately cause cocaine-induced behavioral responses, such as cocaine seeking.